UNIVERSITY OF MINNESOTA
ST. ANTHONY FALLS HYDRAULIC LABORATORY

Project Report No. 72

Further Studies of Ventilated Cavities on Submerged Bodies

by
F. R. SCHIEBE
and
J. M. WETZEL

Prepared for
OFFICE OF NAVAL RESEARCH
Department of the Navy
Washington, D.C.
under
Contract Nonr 710(48), Task NR 062-192

October 1964
Minneapolis, Minnesota

ABSTRACT

This report supplements an earlier report describing experimental studies conducted to determine the air requirements of ventilated cavities on hydrofoils and other submerged bodies in the vicinity of a free surface. Reentrant jet, trailing vortex, and pulsating cavities were observed.

In the present report, primary attention was given to extending an analysis of the type reported by Cox and Clayden and later extended by Campbell and Hilborne for predicting the air requirements of trailing vortex type cavities and for obtaining pertinent experimental data. It was shown that good agreement with the experimental data was obtained by both theoretical and semi-empirical expressions.

Secondary attention was given to further verification of a correlation parameter previously derived for reentrant jet type cavities. The transition region between reentrant jet and trailing vortex cavities was also investigated. For some conditions, pulsating cavities were found in the transition region.

CONTENTS

LIST OF ILLUSTRATIONS

LIST OF SYMBOLS

A - planform area

A_p - vertical projection of area, $A \sin \alpha$

AR - aspect ratio

a - diameter of vortex cores

C_a - concentration of voids by volume, also called correlation parameter

C_D - drag coefficient

C_{D_o} - drag coefficient at zero cavitation number

C_L - lift coefficient

c - hydrofoil chord

c_f - flap chord

d_m - maximum cavity thickness

F_r - Froude number

f - foil submergence

f_p - frequency of pulsation

g - acceleration of gravity

ℓ - average cavity length

n - constant

n_p - stage or number of waves on pulsating cavity

P_a - partial pressure of air in cavity

P_c - cavity pressure

P_v - vapor pressure

Q - volume flow rate of ventilating gas

q_c - peripheral velocity of vortex tubes

R - gas constant for air

R_o - radius of external boundary

r_o - radius of circle filled with gas

s - area of cavity under steady conditions

T - temperature of cavity gas

V - free stream velocity

V_c - velocity at cavity wall

W - weight flow rate of ventilating gas

α - geometric angle of attack

Γ_g - circulation due to gravity

Λ - sweep angle of quarter-chord line

λ - ratio of tip chord to root chord

ρ - fluid density

σ - cavitation number based on average cavity pressure P_c

σ_v - cavitation number based on vapor pressure P_v

σ_{min} - minimum σ obtained by artificial ventilation

FURTHER STUDIES OF VENTILATED CAVITIES ON SUBMERGED BODIES

I. INTRODUCTION

Many problems have arisen with the advent of very high speed hydrofoil craft. Traditionally the naval architect has been confronted with a cavitation problem which limited the speed at which a body could be efficiently propelled through water. The emphasis in solving the problem has been in the prevention of cavitation. This line of approach created a cavitation barrier or a maximum speed beyond which it became uneconomical to operate.

For naval craft, speeds greater than this limit were desired. The development of the supercavitating hydrofoil sections in effect has broken the cavitation barrier and allows craft to travel more economically at speeds much greater than previously possible. The force characteristics of these new sections are such that the performance ratio is maximized when the cavity is fully developed.

It may be desirable to control the cavitation number for some regions of operation. If the cavitation number is too high at a particular speed and depth, the hydrofoil may be in a subcavitating, incipient cavitating, partially cavitating, or buffeting condition where the cavity is only slightly larger than the hydrofoil chord. All of these conditions are undesirable for various reasons.

The control of the cavitation number may be achieved by the introduction of a gas from an external source into the wake region of the hydrofoil, thus creating a fully developed cavity where one would either not normally exist at all or exist in the incipient, partially developed, or buffeting state. By this method a cavity may also be obtained at relatively low velocities. In the experiments described in this report, air was used as the ventilating gas.

The characteristics of such artificially ventilated cavities, with emphasis on the air requirements, will be examined in this paper. It is convenient to discuss the relationship between the air requirements and the cavitation number by referring to two types of cavities. The first type, for which the air requirement is proportional to the cavitation number, is called the re-entrant-jet cavity. The second type, for which the air requirement is

essentially independent of the cavitation number, is identified with formation of trailing vortices due to gravitational effects as well as pulsations of the cavity under some circumstances.

There is a definite transition between the two types of cavities, which is evident in the experimental data and in photographs of the cavity. Observation of the wake region of the cavity attached to a flat plate hydrofoil of aspect ratio 6 shows that small trailing vortices are present even if a strong reentrant jet is the dominant mechanism for eliminating air from the cavity.

Rather extensive studies of reentrant jet cavities behind rectangular flat plate hydrofoils were described in Ref. [1]*. Some additional data for other hydrofoils and bodies are presented in this report. For the most part, the discussion in this report will be devoted to the trailing vortex type cavity.

II. REENTRANT JET CAVITIES

The main mechanism of air entrainment for relatively short cavities is the reentrant jet originating at the rear of the cavity. The jet strikes the walls of the cavity, and air is removed from the cavity by means of a turbulent mixing process. The reentrant jet cavity, while considered a steady flow, is in reality unsteady because of the stochastic fluctuations superimposed on the average steady reentrant jet. This fluctuation in the reentrant jet thus results in the air entrainment having both steady and unsteady components. As this mechanism is very complex, it is advantageous for most purposes to consider the process on an average basis and treat the flow as steady.

In a previous report [1] an expression has been derived for determining the air requirements for reentrant jet cavities. This expression contained an empirical constant derived from measurements made for various bodies. As the equation will be used in this report it is repeated for reference purposes. The air requirements were given by

$$W = \frac{C_a P_a V A C_D}{2(1 - C_a)\left[1 + \sqrt{1 + \sigma}\right] RT} \qquad (1)$$

*Numbers in brackets refer to List of References on page 25.

where W = cavity air-requirement, lbs per sec,

C_a = concentration of voids by volume, also called correlation parameter,

$P_a = P_c - P_v$ = partial pressure of air in the cavity, psfa,

P_c = cavity pressure, psfa,

P_v = partial pressure of water vapor in the cavity, psfa,

V = free stream velocity, fps,

A = planform area of the body, sq ft,

C_D = drag coefficient (cavity drag),

σ = cavitation or ventilation number based on average cavity pressure, P_c,

R = gas constant for air = 53.3 ft lbs per lb per degree Rankine, and

T = gas temperature in cavity, degree Rankine.

C_a was determined experimentally for various bodies by measuring all the other factors in the equation. An empirical relationship relating C_a to σ and aspect ratio was found to satisfactorily correlate the available data.

Part of the effort of the present experimental program was devoted to an extension of the previously reported experiments to determine the concentration of the voids as a correlation parameter in analyzing the air demand data for reentrant jet cavities.

In the report, the terms "concentration of voids" and "correlation parameter" will be used interchangeably. In the reported experiments, a wide variety of body shapes were used, including flapped hydrofoils and hydrofoils with non-rectangular planform and non-lifting flat plates. A description of the experimental apparatus, test bodies, and procedure is included in the Appendix.

Since the drag coefficient was found to be an important parameter in the study of the air requirements for cavities, the forces on the various bodies were measured. The force data for the flapped foils were analyzed in a previous study conducted at this Laboratory and were presented in Ref. [2]. The drag coefficients which were used in the present computations of the correlation parameter were taken from that source. Additional force data obtained with a non-rectangular planform foil and a normal flat plate are shown in Fig. 1. The normal flat plate was oriented so that the 0.369 in. dimension was perpendicular to the flow. As indicated in the Appendix, the submergence, f,

was measured from the leading edge of the foil to the free water surface. The angle of attack, α, was taken as the angle between the velocity vector and the under surface of the foil.

The drag data for the normal flat plate at small cavitation numbers were expected to fall close to the curve calculated from

$$C_D = C_{D_{\sigma = 0}} (1 + \sigma) \tag{2}$$

The value of $C_{D_{\sigma = 0}}$ from the two-dimensional hydrodynamic theory for a normal flat plate is 0.88. The present experiments indicate a value of $C_{D_{\sigma = 0}} = 0.785$ for an aspect ratio of 32. The ratio of the two-dimensional to the three-dimensional drag coefficients corresponds approximately to the value obtained from measurements taken in wind tunnels for the same body.

Plots of the air flow requirements vs. cavitation number are shown in Figs. 2 and 3 for the non-rectangular planform foil and the normal flat plate, respectively. These data, as well as data for a foil with a trailing edge flap and a foil of aspect ratio 2 presented in Fig. 4, have been reduced in terms of the concentration parameter, C_a. As additional data for larger and smaller aspect ratio foils became available, it appeared that the dependence of C_a on aspect ratio was less significant than first implied. It was thus possible to reasonably express the concentration parameter as a function of σ alone. This relation was written as

$$C_a = 0.59 - 0.83\ \sigma$$

which corresponds to the empirical expression previously given in Ref. [1] evaluated at an aspect ratio of 6. Equation (3) has been plotted in Figs. 2, 3, and 4 and it will be noted that this expression fits the experimental data quite well, even for flapped foils with flap angles up to 20 degrees. The latter data were for a flap-chord ratio, c_f/c, of 0.25. Equation (3) has been substituted in Eq. (1) to calculate the air flow requirements for the normal flat plate, and the results are shown by a broken line in Fig. 3a. Considerable scatter exists in the experimental data in this case, particularly for cavitation numbers between 0.08 and 0.16.

Very long transients in the cavity characteristics were found for this particular range of cavitation numbers. The cavity pressure did not attain a constant value in the available test run. Various methods were used to ventilate the cavity and it was found that if the air was supplied after the desired test speed was attained, the transient was much reduced in the cavitation number range of 0.14 to 0.2. For the longer cavities, better results were obtained with the air supplied before the carriage was started. Various proportions of air supplied before the carriage was started and after constant speed was reached produced fairly successful results. The calculated curve represents roughly an average of these conditions.

The relationship between air flow rate and cavitation number was dependent on the type of cavity for the range of velocities used in these tests. For reentrant jet cavities, an increase in velocity required an increase in air flow to maintain a constant σ. If the air flow rate was held constant, the cavitation number increased and the cavity length decreased with increasing velocity. For non-reentrant jet cavities, the opposite trend was found to exist. Thus, if a long stable cavity was desired, providing a large air flow at the start of the test run resulted in a cavity shorter than necessary; this cavity would increase in size as the velocity increased. If a short cavity was desired, setting the air flow rate at the start of the test run resulted in an initial cavity considerably longer than necessary. The time required for the cavity pressure to attain a constant value was much longer in the latter case, and it was therefore concluded that transients associated with a collapsing cavity were of more significance than for a developing cavity. These effects are currently being investigated more fully in conjunction with other studies on unsteadiness effects, and will be discussed in a separate report.

In addition to the work previously discussed, an effort was made to correlate, with the same concentration parameter, air entrainment rates obtained under quite different flow conditions in the laboratory free jet water tunnel. Reference [1] has shown that the air entrainment rates for bodies in the free jet were substantially higher than those for similar bodies tested in the towing tank.

There are two main differences concerning the tests in the towing tank and the vertical free jet tunnel. The direction of the gravity field in the towing tank is normal to the longitudinal axis of the cavity, while in the vertical free jet it is parallel to the longitudinal axis of the cavity. In

the free jet there are two free surfaces, one on each side of the hydrofoil cavity system, while in the towing tank there is only one. The presence of the free surfaces influences the force coefficients to some extent, particularly in the case of the free jet. This, however, is taken into account in the calculation of the correlation parameter by using the measured drag coefficient.

The direction of the gravity field produces a significant difference in the behavior of the reentrant jet. In a horizontal cavity the jet enters from the rear and falls until it strikes the lower surface of the cavity. At the intersection of the reentrant jet and the lower surface, the ventilating gas is entrained and swept to the rear of the cavity and is thus lost from the cavity. In a vertical cavity the reentrant jet contacts both cavity walls, thus making both cavity walls effective in eliminating gas from the cavity. It will now be shown that the air demand for vertical cavities is approximately twice that for horizontal cavities. Equation (1) may be modified by a factor, n, which specifies the number of cavity walls effective in eliminating cavity gas. In the case of a horizontal cavity in a towing tank, $n = 1$, whereas in the case of a vertical cavity in a free jet, $n = 2$. The modified Eq. (1) now becomes

$$W = \frac{nC_a P_a VAC_D}{2(1 - C_a)\left[1 + \sqrt{1 + \sigma}\right] RT} \tag{4}$$

or

$$C_a = \frac{K'}{1 + K'} \tag{5}$$

where

$$K' = \frac{2W(1 + \sqrt{1 + \sigma})\, RT}{nP_a VAC_D}$$

To determine the validity of this modification, additional data were taken in the free jet tunnel with a flat plate foil of 2 in. chord and aspect ratio of 2.5. The force data and the concentration parameter reduced from the measured air flow rates are shown in Fig. 5. The velocity for these tests varied from about 25 to 44 fps, as indicated in the legend. The agreement of the data with Eq. (3) is satisfactory.

In a final attempt to establish the validity of Eq. (3) and its usefulness in the prediction of air entrainment rates, data for a wide range of conditions have been plotted in Fig. 6a. These data were taken for various lifting and non-lifting bodies with aspect ratios varying from 2 to 32. A number of angles of attack, flap angles, and submergences were included. The points shown do not represent all the experimental data accumulated, but are typical of those obtained. The solid line drawn through the data has been determined from Eq. (3). The two dashed lines represent a $\pm$10 per cent variation from the empirical curve. The bulk of the data lie within these extremes. Analysis of the data indicated that about $\pm$2 per cent of the deviation could be attributed to reading errors in the instrumentation system. It will be recalled that the air entrainment rates are directly proportional to $\frac{C_a}{1 - C_a}$. Considering a $\pm$10 per cent deviation in C_a, the error of using this method for calculating the air entrainment is shown in Fig. 6b as a function of the cavitation number.

Another method of presenting data for ventilated cavities which has been utilized by other investigators groups the rate of air flow, velocity, and the vertical projection of the wetted hydrofoil area in the dimensionless parameter $W/A_p V$. When the data of the current program were plotted in this form against the cavitation number, a maximum deviation was found of $\pm$47 per cent of $W/A_p V$ based on the mean value at a cavitation number of 0.2. This error is much greater than the $\pm$17 per cent deviation shown in Fig. 6b for the same cavitation number. This seems to indicate, for the data taken at this Laboratory, that the use of the concentration of voids as a correlation parameter is a definite improvement over the correlation parameter defined by $W/A_p V$.

III. TRAILING VORTEX CAVITIES

As the gas supply rate to the cavity is increased, a point is reached where another mechanism for eliminating gas from the cavity is dominant over the reentrant jet, which, although present, is relatively weak, and the cavitation number is practically independent of the gas supply rate to the cavity. Rather large trailing vortices appear at the rear of the cavity due to gravitational circulation about the cavity. These vortices occur in pairs and are noted in addition to the tip vortices which are produced by lift of the finite span foil. The cavity vortices can be observed more readily in

cases where the tip vortices are relatively weak. The trailing vortices are apparent as air-filled tubes far downstream of the cavity tail in Fig. 7a for a cambered foil equipped with circular end plates. The origin of the tubes can also be seen at the tail of the cavity. Under some conditions, the cavity displayed a periodic pulsation phenomenon. An example of pulsation is shown in Fig. 7b for the same foil with a slightly lower quantity of air supplied to the cavity. This pulsation phenomenon will be neglected in the following discussion. It should be noted, however, that even in the presence of cavity pulsation, some resemblance of the trailing vortices is present far downstream of the cavity.

The existence of vortex tubes at the higher air-flow rates was found in previous investigations of ventilated cavities conducted at the California Institute of Technology [4] to determine the air entrainment behind a circular disk submerged below a free surface. In these studies it was found that as the air-flow rate was increased the cavity changed from a reentrant jet to a trailing vortex type cavity. Cavity pulsations were apparently not observed.

Subsequent tests of the same nature were performed by Cox and Clayden [5] and later by Campbell and Hilborne [6]. A theory based on aerodynamic theory, which determined the size of the trailing vortex tubes, has been developed by the former authors and extended by the latter.

It was assumed that since the cavity pressure remains essentially constant throughout the cavity, the velocities on the upper and lower walls of the cavity must differ because of the hydrostatic pressure difference on the cavity walls. This gave rise to a circulation which permitted an approximation to the size of the vortex tubes. The tubes served as pipes through which the gas was carried away from the cavity.

The approach utilized in Refs. [5] and [6] will be followed here with some minor modification to make the results consistent with the physical conditions of the current tests.

The cavity is approximated in the vertical meridian plane by an ellipse and, following a linearized approach, the circulation set up by the gravitational field is

$$\Gamma_g = \frac{g\pi}{4V} d_m \ell \qquad (6)$$

where Γ_g = gravitational circulation in sq ft per sec,
g = acceleration due to gravity = 32.2 ft per sec^2,
d_m = maximum cavity thickness in ft, and
ℓ = cavity length in ft.

The transverse velocity, q_c, around the periphery of the vortex tubes is, by application of Bernoulli's equation, given by

$$q_c = V\sqrt{\sigma} \tag{7}$$

The diameter of the vortex cores is then given by

$$a = \frac{\Gamma_g}{\pi q_c} \tag{8}$$

or

$$a = \frac{g d_m \ell}{4V^2\sqrt{\sigma}} \tag{9}$$

According to Campbell and Hilborne the volume of gas needed to be supplied to the cavity to maintain a constant cavitation number is given by

$$Q = 2\left(\frac{\pi a^2}{4}\right)V \tag{10}$$

or to be consistent with the nomenclature of this paper by

$$W = \frac{\pi g^2 P_a d_m^2 \ell^2}{32\,RT\,V^3\,\sigma} \tag{11}$$

for each pair of vortex tubes. In the experiments with the circular disks of Refs. [5] and [6], only one pair of tubes was observed.

Visual observations of the cavity and photographs taken in the present study of lifting hydrofoils indicate that the number of pairs of the trailing vortices present is not only one as observed in the experiments with the circular disks, but depends a great deal on the aspect ratio of the body. For high aspect ratios several pairs of vortex tubes have been noted. For low aspect ratios (AR = 2.5 or less) there seems to be only one pair present. In general the phenomenon appears to be quite complex.

Part of the problem of determining the air demand for such cavities is thus reduced to determining the number of pairs of vortices and the cavity dimensions in the vertical-longitudinal planes where each pair of vortices leaves the main cavity.

The three-dimensional effect on the cavity characteristics is shown in the photograph of Fig. 8 for a typical flow condition. In this particular case of a 3- by 18-in. flat plate hydrofoil, several of the previously described trailing vortices are seen leaving the cavity. The outermost pair are, of course, the tip vortices due to the lift and finite span of the hydrofoil. The direction of rotation of these tip vortices has been observed to be opposite to those in the interior flow field. It is obvious from this photograph that the cavity length is different at the points where each pair of vortices leaves the cavity. It can be presumed that the maximum cavity thickness also changes in a spanwise direction across the cavity. Experimental data concerning the cavity dimensions were determined from photographs similar to Fig. 8.

Information relative to the cavity dimensions is available from the non-linear theory by Wu [7] for a two-dimensional cavity in an infinite fluid. In this analysis, the cavity length, ℓ, and maximum thickness, d_m, are given by

$$\ell = \frac{4cC_D}{\pi\sigma^2\left(1 + \sigma + \frac{\epsilon^2}{6}\right)} \tag{12}$$

$$d_m = \sigma\,\ell \tag{13}$$

where c = chord in ft and

$\epsilon = 1/2\ \ell n\ (1 + \sigma)$.

For cavitation numbers in the range of interest ($\sigma < 0.15$), it was assumed that $C_D = C_{D_o}\ (1 + \sigma)$. For small σ, the quantity $\epsilon^2/6$ is much less than unity and can therefore be neglected. The expression for the cavity length then reduces to

$$\ell = \frac{4cC_{D_o}}{\pi\sigma^2} \tag{14}$$

This equation may be made dimensionless by rearranging it into the form of a reduced cavity length,

$$\frac{\ell}{cC_{D_o}} = M\sigma^{-n} \tag{15}$$

where $M = 4/\pi$, and

$n = 2$

are the theoretical values from the two-dimensional, non-linear theory by Wu.

Experimental data were analyzed to determine M and n for three-dimensional foils and various conditions. The values of C_{D_o} were computed by Johnson's method [11] which has been experimentally well verified. The cavitation number varied between 0.05 and 0.4, the submergence from 0.5 to 3 chords, and the angle of attack from 8 degrees to 20 degrees for these experiments.

The reduced cavity length, as expressed by Eq. (15), was plotted against the cavitation number on logarithmic paper and it was found that a straight line of the form of Eq. (15) could be fitted to the experimental data. M was found to change with angle of attack, submergence, and aspect ratio while the value of n scattered slightly about unity. Since this scatter was small, n was taken equal to unity and the coefficient, M, was revaluated.

The fact that the cavity length depended inversely on the first power of the cavitation number rather than the second power as predicted by the non-linear theory was of some interest. It was first thought that this trend was an effect of finite span since the cavity length for axi-symmetric bodies is proportional to $1/\sigma$. However, reexamination of the data taken in the free jet water tunnel [12] for the cavity length of two-dimensional foils showed that the length data were better represented by an inverse first power of cavitation number in this case also. It may be possible that the influence of the free surfaces reduced the power of the cavitation number.

Figure 9 shows some cavity length data for an aspect ratio 2.5 flat plate hydrofoil compared to curves varying inversely with the cavitation number. The length was measured from the leading edge of the foil to the extreme tail of the cavity. Further reduction of the data showed that for a given submergence and aspect ratio the coefficient M was proportional to

some power of the angle of attack and the submergence. The resulting empirical relationships for an aspect ratio 2.5 hydrofoil are

$$M = \frac{169\ f^{0.32}}{\alpha^{1.2}} \tag{16}$$

where f = submergence in chords, α = angle of attack in degrees, and

$$\frac{\ell}{cC_{D_o}} = \frac{169\ f^{0.32}}{\alpha^{1.2}\ \sigma} \tag{17}$$

The solid curves through the data plotted in Fig. 9 were calculated using Eq. (17). For purposes of comparison, points computed from the non-linear theory (length varies with the inverse square of the cavitation number) are also plotted. It can be seen that the agreement between these curves [Eq. (15)] and the data is not satisfactory.

There were insufficient data available to determine similar generalized expressions for the aspect ratios of 4 and 6. However, the available data for a few specific conditions are presented in Table I below.

TABLE I

$$\frac{\ell}{c} = (MC_{D_o})/\sigma^n \quad (n = 1.0 \text{ Assumed})$$

AR	α degrees	M			Foil Dimensions inches
		f = 1c	f = 2c	f = 3c	
2.5	8	13.60	17.10	No data	3 by 7.5
2.5	10	10.51	11.49	12.44	3 by 7.5
4.0	10	11.77	14.17	14.35	3 by 12
6.0	10	12.12	15.62	16.53	3 by 18
2.5	12	8.22	12.00	12.48	3 by 7.5
2.5	14	6.89	8.56	9.93	3 by 7.5
4.0	14	9.17	9.75	No data	3 by 12
6.0	14	8.36	9.86	10.74	3 by 18
2.5	16	5.77	7.62	8.27	3 by 7.5
2.5	18	5.01	6.31	7.70	3 by 7.5
6.0	18	6.36	7.79	No data	3 by 18
2.5	20	4.06	5.55	5.78	3 by 7.5

For small aspect ratio hydrofoils the trailing vortices leave very close to the extreme rear of the cavity and the empirical cavity length given by Eq. (17) may be used in Eq. (11).

As previously noted, Wu's [7] non-linear analysis resulted in a value of the cavity slenderness ratio, d_m/ℓ, equal to the cavitation number. The various linearized developments indicate that the slenderness ratio is equal to the cavitation number divided by 2. Measurements based on photographs taken of cavities in the free jet water tunnel and on photographs presented in Ref. [8] show that at small cavitation numbers ($\sigma < 0.15$) the slenderness ratio for two-dimensional cavities is approximately equal to the cavitation number.

For three-dimensional cavities, however, the observed slenderness ratio was greater than the cavitation number. Reichardt's data [9] for cavities on axi-symmetric bodies indicate a slenderness ratio of 2.18σ at $\sigma = 0.1$. Limited measurements in the free jet water tunnel indicate that for an aspect ratio 2.5 flat plate hydrofoil, the slenderness ratio is roughly 2σ at low cavitation numbers.

If the cavity length from Eq. (15) and the experimentally observed slenderness ratio of 2σ are substituted into Eq. (11) for the air requirements, the following expression is obtained for low aspect ratio hydrofoils ($AR = 2.5$ or less) where only one pair of trailing vortices has been observed.

$$W = \frac{\pi g^2 c^4 C^4_{D_o} M^4 P_a}{8V^3\sigma^3 RT} \tag{18}$$

The coefficient M can be obtained directly from Eq. (16). Equation (18) can be further reduced by expressing $P_a = P_c - P_v$, and $P_c = P_\infty - \frac{1}{2}\rho V^2 \sigma$ as was done in Ref. [1] in developing the air demand for reentrant jet cavities. The final result is

$$W = \frac{\pi g^2 c^4 C^4_{D_o} M^4 \rho}{16 V \sigma^3 RT} [\sigma_v - \sigma] \tag{19}$$

per pair of vortex tubes. Here σ_v is the cavitation number based on vapor pressure.

In Fig. 10a, Eqs. (4) and (18) are compared with data taken with a 2.5 aspect ratio flat plate hydrofoil of 4-in. chord. The test conditions are noted on the figure. Figure 10b shows a comparison of data taken with a 2.5 aspect ratio flat plate hydrofoil of 3-in. chord with Eqs. (4) and (18).

The intersection of the two curves agrees quite well with the transition from reentrant jet to non-reentrant jet cavities. Cavity pulsations did not occur for the tested condition in the case of the 4-in. chord hydrofoil and occurred inside the indicated region on Fig. 10b in the case of the 3-in. chord foil.

It was also of interest to determine the sensitivity of Eq. (11) to slenderness ratio and cavity length. Therefore, the theoretical two-dimensional infinite fluid values of $M = \frac{4}{\pi}$ and the inverse square of the cavitation number were used in computing cavity length, and the slenderness ratio was taken equal to σ. The resulting expression is

$$W = \frac{8g^2 c^4 C_{D_o}^4 P_a}{\pi^3 V^3 \sigma^7 RT} \tag{20}$$

Equation (20) is also plotted in Fig. 10. It can be seen that the intersection of Eq. (20) and Eq. (4) also agrees fairly well with the lowest σ for which reentrant jet cavities were observed.

Examination of these plotted curves of Eqs. (18), (19), and (20) shows that the calculated slopes of the W versus σ curve are very steep in the region of applicability. W is inversely proportional to the velocity and W also is directly proportional to the number of pairs of vortices involved if all pairs were assumed to carry the same amount of air. All three of these trends have been observed experimentally. At very high speeds when σ_v approaches or is equal to σ, the air demand approaches or is equal to zero as expected.

It can also be seen in Fig. 10b that when the values of M and C_{D_o} for the various submergences are inserted into Eq. (18), the effect of submergence on the minimum cavitation number is shown quite accurately. Wu's values, based on a theory for an infinite fluid were used in Eq. (20); therefore this equation provides no information as to the influence of a free surface. For comparison, the dashed curve in Fig. 10a was computed using M and C_{D_o} for the indicated flow conditions of the test.

The application of this type of analysis to larger aspect ratio foils is as yet uncertain. On three-dimensional cavities the cavity length varies along the span as observed in Fig. 8. It is evident that the length in any given plane on a three-dimensional cavity must be a function of aspect ratio and distance from the center along the span as well as c, C_{D_o}, and σ as

indicated by Eq. (12). It is the length where the vortex tubes in question depart from the cavity which probably should be used in Eq. (11) to compute the weight rate of air lost through the pair of vortices leaving the cavity in that location. The problems of finding exactly where these vortices will leave the cavity and of determining the number of pairs that will leave the cavity are as yet unresolved.

The influence of the free surface on the air entrainment rates for trailing vortex cavities was determined by another method. Experimental data indicate that the actual slope of the air demand versus cavitation number curve is even steeper than predicted by Eq. (18) or Eq. (20). There appears to be a minimum cavitation number, for given conditions, below which further reduction cannot be achieved by artificial ventilation. This minimum cavitation number is considerably influenced by the submergence of the body. After obtaining the general trends of this behavior from curves such as those presented in Fig. 10b, extensive data were taken with an air injection rate sufficiently large so that the resulting cavities would not pulsate. The resulting data on the minimum σ for several velocities and chords were found to be correlated well by the product of cavitation number and the Froude number based on the vertical projection on the chord, $c \sin \alpha$.

The dependence of $F_r\sigma_{min}$ on submergence and its relative independence of velocity and angle of attack is shown in Fig. 11. Plotted in the figures is also an empirical expression given by

$$F_r\sigma_{min} = K(1 - e^{-1.66f}) \tag{21}$$

where

$$F_r = \frac{V}{\sqrt{gc \sin \alpha}}$$

σ_{min} = minimum σ obtained by forced ventilation,
f = foil submergence in chords, and
K = some function of aspect ratio.

Experiments conducted with foils of various aspect ratios have shown that the constant, 1.66, does not vary with aspect ratio, while the constant K varied as indicated in Table II.

TABLE II

Aspect Ratio	K
2.5	0.86
4	0.95
6	0.733

Using Eq. (21), fairly good estimates can be made regarding asymptotic values of the air demand curves. Accurate predictions in the region of interest are very difficult due to the very steep slope of the curve.

IV. PULSATING CAVITIES

For the tests conducted in the towing facility, with finite span foils, cavity pulsations may or may not occur in the transition region between reentrant jet cavities and trailing vortex cavities. Considerable effort has been expended to determine both experimentally and theoretically the conditions under which cavities will pulsate. However, the complete solution of this problem is still unavailable.

The cavity pulsation phenomenon was first observed experimentally by Silberman and Song [12] on bodies in a vertical free jet water tunnel. In this vertical facility the gravity effects, which produced a pressure difference across the cavity in the towing tank, were not present and therefore trailing vortices were absent. The cavity progressed from a reentrant jet cavity to a pulsating cavity under any and all conditions as the air flow rate into the cavity is increased.

Another observation of pulsating cavities was noted in towing experiments and was described in Ref. [1]. The principal difference between the results from the two facilities was in the gravitational effects on the horizontal cavities in the towing tank. These gravitational effects proved to be dominant when a sufficient supply of air was injected into the cavity. Under these conditions the cavity pulsations are regarded as a transition phenomenon. However, as described in Ref. [1] the cavity pulsations did not occur in the transition region under all circumstances. The angle of attack and the hydrofoil chord length seemed sensitive parameters in determining whether or not the pulsation would occur. In general, under conditions which produce thin cavities such as low angles of attack and small chord lengths, pulsation of the cavity would occur. At larger attack angles and chords, the cavity progressed directly from a reentrant jet to a trailing vortex cavity with

increasing air injection rates without exhibiting any pulsations. Higher towing velocities also seemed to reduce the tendency for a cavity to pulsate. For reference purposes, the data of Ref. [1] are presented in Fig. 12. Some additional data taken with the non-rectangular planform have also been added. Each of the curves for a given parameter, such as velocity, indicate a pulsation threshold. Cavities pulsated on ventilated hydrofoils operating at angles of attack below the curve for a given parameter. Foils operating at attack angles above the curve did not exhibit cavity pulsation in the transition region. It will be recalled that Figs. 10a and 10b show conditions for which pulsations are not or are occurring respectively, in the transition between reentrant jet and trailing vortex type cavities.

Theoretical work concerning the stability of ventilated cavities has been performed by Song [13] and by Hsu and Chen [14].

In the analysis by Song, the kinematical requirements of the pulsating cavity were matched to the solution of the dynamical model. His dynamical model consisted of an annulus. The core of the annulus represented the cavity, and the annular distance between the inner and outer walls represented the surrounding water in the free jet system. The area outside the annulus represented the atmosphere into which the free jet was discharging. This model, although considerably simplified, was analyzed in terms of a mass-compliance system, in which the damping terms were neglected.

Information for the kinematical model was obtained from experimental evidence which has shown that a number of waves appear on the cavity and travel with the flow along the cavity surface.

Song determined the number of wave lengths on the cavity as

$$\frac{f_p}{V_c} = n_p \tag{22}$$

for sustained cavity oscillations.

The frequency of the waves must match the resonant frequency obtained from the dynamic model. This frequency was determined as

$$f_p = 0.473 \sqrt{\frac{P_a}{K_1 \rho s \, \ell n \frac{R_o}{r_o}}} \tag{23}$$

where K_1 = constant,

R_o = radius of external boundary,

r_o = radius of circle filled with gas,

s = area of cavity for steady conditions, and

f_p = frequency of pulsation.

Song concluded from his analysis that the pulsation phenomenon is associated with a free surface. Since the volume of the cavity changes with time, it follows that in an incompressible infinite fluid or in a closed chamber the volume of the water must change. Thus, if the water is assumed incompressible, cavity pulsations will not occur. A free surface, however, will allow the total space occupied by the cavity-water system to change; thus cavity pulsations can occur. All known visual observations of cavity pulsation have been in the close vicinity of a free surface.

Hsu and Chen have attempted to show theoretically that the compressibility of water is sufficient to permit cavity pulsations even in an infinite fluid. In their analysis the change in volume of the cavity calculated by considering the interaction of the streaming flow and the cavity was matched to the volume calculated by an appropriate gas law. Experiments to verify this theoretical result have not yet been performed. In addition to the ability of a ventilated cavity to pulsate in an infinite fluid, their results indicate that the occurrence of resonance involves properties of the gas in the cavity and the flowing liquid and not the size of the body itself. In the towing tank experiments where gravity is an important factor, the body size, however, was shown to have an influence on the initial stability of the cavity as previously discussed.

The available data relative to pulsating cavities have been previously correlated by plotting the cavitation number based on measured cavity pressure against the cavitation number on vapor pressure. This has been the technique used in Refs. [1], [12], and [13]. The semi-empirical equation developed by Song [13] agrees with the data quite well. This equation is given by

$$\sigma_v = (1 + 3.45\, n_p^2)\, \sigma + 3.45 n_p^2 \sigma^2 \qquad (24)$$

The constant 3.45 is determined basically from the physical flow parameters.

It was also of interest at this time to compare Hsu and Chen's calculated results reduced to the form of a σ versus σ_v plot. This comparison is shown in Fig. 13 together with experimental data collected from tests conducted in the free jet tunnel and the towing tank facility. A number of curves are presented in this plot. The solid lines were plotted from Eq. (24). As n_p is the number of waves on the cavity, it must be an integer, and different curves are obtained for each particular value of n_p. The number of waves is indicated at the upper limit of each curve. The dashed lines have been plotted from an empirical equation first presented in Ref. [12]. Theory by Hsu and Chen results in curves shown by the long and short dashed line.

In general, it will be noted that the semi-empirical equation by Song [13] agrees quite well with both the experimental data and the fully empirical equation by Silberman and Song [12]. It should also be mentioned that the experimental data obtained from the towing tank experiments for the higher values of σ_v may be in error by plus or minus one wave length. The number of waves were determined from photographs of the cavity, and the cavity may or may not have been just pinched off at the instant the photo was taken.

The theory by Hsu and Chen results in two sets of curves for each assumed number of waves on the cavity. A critical value was found at a ratio of cavity length to chord length of 4, and this condition is represented by the curve appropriately labeled. The predicted trends do not appear to be reflected by the experimental data. Reentrant jet cavities were generally observed at any cavitation number above the data shown in Fig. 13. The uppermost curves which lie above the $\ell/c = 4$ curve as computed by Hsu and Chen would therefore lie in the reentrant jet regime.

An examination of the photos of pulsating cavities in the vertical free jet water tunnel presented in Ref. [12] indicated that the amplitude of the surface waves on both cavity walls was essentially the same for symmetrical bodies and of the same order of magnitude in the case of an unsymmetrical body such as a lifting hydrofoil. It was of interest to determine whether or not such a behavior existed for a foil moving horizontally beneath a free surface. Several tests were consequently conducted in the towing facility with foils at both positive and negative angles of attack. Photographs were taken of the cavity from beneath the water surface. Typical photos are shown in Fig. 14. Figure 14a shows a pulsating cavity attached to a flat plate foil at a positive angle of attack of 12 degrees and moving from right to left at

a velocity of 12 fps. The foil submergence was 2.5 chords and the foil had an aspect ratio of 2.5. The top image in this photograph shows the upper surface of the cavity, as reflected by the free water surface. Definite cavity pulsations or waves of large amplitude can be observed, particularly near the rear of the cavity. The underside of the cavity, as seen in the lower image, appears to be free of any well defined wave.

The same foil was then modified to permit the introduction of air to its under surface, and the foil was placed at a negative angle of attack of 12 degrees, so that the pressure side of the foil was nearest the free water surface. A photo of the resulting cavity with the other conditions remaining the same is shown in Fig. 14b. Several differences in the cavity characteristics are to be noted. It is now apparent that waves exist on both cavity walls. Also, the cavity planform is more two-dimensional in shape. The tail of the cavity is almost parallel to the leading edge of the foil, whereas in the case of the foil at the positive angle of attack, the cavity tail becomes more rounded. This effect is further emphasized in Fig. 15. The photos in Fig. 15 were taken from above the cavity and through the free surface. The upper photos were taken with the foil at a negative angle of attack, and the lower photos with the foil at a positive angle of attack. The difference in cavity planform exists for both pulsating and non-pulsating cavities.

The appearance of waves on the underside of the cavity raises some questions concerning the role of the free surface in the pulsation phenomenon. More work, both experimental and theoretical, is necessary to arrive at a satisfactory solution to the problem.

V. VENTILATION CHARACTERISTICS AT LOW ANGLES OF ATTACK

Difficulty has been experienced at this laboratory as well as at other laboratories in obtaining stable, force-ventilated cavities at low angles of attack and low velocities. As shown in Fig. 1A of the Appendix, the foils used in the current investigation were of wedge cross-section with a 6 degree wedge angle. The leading edge was sharp. It should also be noted that an auxiliary air port was provided very close to the leading edge of the foil, in an attempt to achieve ventilation more readily by supplying air into the separated zone in that area. Furthermore, the air jet may in turn stimulate a boundary layer separation. This method was partially successful, although even with this artifice, the lowest angle of attack at which a stable cavity

could be initiated and maintained throughout the available test run was about 8 degrees. Photographs have been taken of the cavity under these conditions, and several typical photos are presented in Fig. 16 to indicate the general behavior of the cavity. The first four photos were taken with the foil moving at a velocity of 12 fps. The air flow rate to the cavity was increased in each successive run. The last two photos were taken at a towing velocity of 18 fps.

Observation of the cavity in Fig. 16a will indicate that the cavity does not spring uniformly from the leading edge across the span. Furthermore, the inflated tip vortices are not attached to the tips on the upper surface of the foil, but appear to be emanating from the trailing edge. A portion of the top surface of the foil near the tips remains wetted. A slight increase of the air flow rate results in a pulsating cavity, Fig. 16b, although part of the foil is still wetted. At times it was not possible to obtain a cavity from the leading edge, even at higher air flow rates, as seen in Fig. 16c. The air is swept back and the cavity initiates at the blunt base of the wedge. It can be seen that the supplementary air supply to the leading edge resulted in an inflated region restricted to the immediate vicinity of the supply port, and no full cavity was obtained. With an additional increase in the air flow rate, the air ejecting from the main ports at the junction of the strut and foil disturbs the relatively thin cavity. The beginning of this disturbance can be seen in Fig. 16d. Larger air flows result in a more or less complete interference with the upper surface of the cavity, and these conditions have been excluded from further consideration. In general, a smoother cavity can be obtained at a higher velocity as shown in Fig. 16e. However, a wetted region still remains at the tips of the foil. A pulsating cavity is shown in Fig. 16f for higher air flow rates. The problem of ventilation at low angles of attack is currently being studied in detail in this laboratory under different contracts.

VI. CONCLUSIONS

(1) Air requirements for hydrofoils with reentrant jet cavities can be computed by

$$W = \frac{nC_a P_a A C_D}{2(1 - C_a)\left[1 + \sqrt{1 + \sigma}\right] RT} \qquad (4)$$

(2) The correlation parameter, C_a, has been determined empirically as

$$C_a = 0.59 - 0.83\,\sigma \tag{3}$$

It was shown that the air requirements for a great number of different types of supercavitating bodies and hydrofoils operating under a variety of flow conditions with reentrant jet cavities can be satisfactorily predicted by the appropriate use of the above equations.

(3) An empirical expression for the cavity length for low aspect ratio hydrofoils (less than 2.5) has been determined as

$$\frac{\ell}{c} = \frac{169\, f^{0.32} C_{D_o}}{\alpha^{1.2}\,\sigma} \tag{17}$$

This expression was obtained from experimental data with the cavitation number varying from 0.05 to 0.4, submergence from 0.5 to 3 chord lengths, and angle of attack from 8 to 20 degrees.

(4) Limited data taken in the free jet water tunnel indicate that the slenderness ratio (ratio of cavity thickness to cavity length) for low aspect ratios (less than 2.5) is roughly 2σ at low cavitation numbers.

(5) A reasonable approximation of the air requirements for trailing vortex cavities can be obtained from

$$W = \frac{\pi g^2 c^4 C_{D_o}^4 M^4 P_a}{8 V^3 \sigma^3 RT} \tag{18}$$

(6) The intersection of Eq. (18) and Eq. (4) satisfactorily predicts the transition between reentrant jet and trailing vortex cavities.

(7) The product of the Froude number, based on the vertical projection of the chord, and the minimum cavitation number is a function of the foil submergence and aspect ratio [Eq. (21)]. The minimum cavitation number is the smallest value obtained by artificial ventilation.

(8) For a body moving horizontally beneath a free surface, the phenomenon of cavity pulsation appears to occur only in the transition region between reentrant jet cavities and trailing vortex cavities. The determination of the exact conditions necessary for a forced-ventilated cavity to become unstable and pulsate has not yet been possible.

ACKNOWLEDGEMENTS

Acknowledgement is given to the various members of the Laboratory staff who have been involved in the collection and reduction of the experimental data. The efforts of L. Boyer in this regard are particularly appreciated. Preparation of the manuscript for printing was carried out by Kathleen Lagerberg, Marjorie Olson, and Pat McNelly.

LIST OF REFERENCES

[1] Schiebe, F. R. and Wetzel, J. M., Ventilated Cavities on Submerged Three-Dimensional Hydrofoils, University of Minnesota, St. Anthony Falls Hydraulic Laboratory, Technical Paper No. 36, Series B, December 1961.

[2] Wetzel, J. M. and Maxwell, W. H. C., Force Characteristics of Flapped, Ventilated Hydrofoils in Smooth and Rough Water, University of Minnesota, St. Anthony Falls Hydraulic Laboratory, Project Report No. 66, January 1963.

[3] Wetzel, J. M., Tandem Interference Effects for Non-cavitating and Supercavitating Hydrofoils, University of Minnesota, St. Anthony Falls Hydraulic Laboratory, Technical Paper No. 50, Series B, in preparation.

[4] Swanson, W. M. and O'Neill, J. P., The Stability of an Air Maintained Cavity Behind a Stationary Object in Flowing Water, California Institute of Technology, Hydrodynamics Laboratory (unpublished).

[5] Cox, R. N. and Clayden, W. A., "Air Entrainment at the Rear of a Steady Cavity," Proceedings of N. P. L. Symposium on Cavitation in Hydrodynamics, London, H. M. S. O., 1956, Paper 12, pp 1-19.

[6] Campbell, I. J. and Hilborne, D. B., "Air Entrainment Behind Artificially Inflated Cavities," Second Symposium on Naval Hydrodynamics, Washington, D. C., August 25-29, 1958, pp 467-480.

[7] Wu, T. Yao-Tsu, "A Free Streamline Theory for Two-Dimensional Fully Cavitated Hydrofoils," Journal of Mathematics and Physics, Vol. XXXV, No. 3, October 1956, pp. 236-265.

[8] Dawson, Thomas Emmett and Bate, E. R., Jr., An Experimental Investigation of a Fully Cavitating Two-Dimensional Flat Plate Hydrofoil Near a Free Surface, California Institute of Technology, Hydrodynamics Laboratory Report No. E-118.12, October 1962.

[9] Reichardt, H., The Laws of Cavitation Bubbles at Axially Symmetrical Bodies in a Flow, Ministry of Aircraft Production, Reports and Translations, No. 766, August 15, 1946, (distributed by Office of Naval Research, Washington, D. C.).

[10] Self, Morris W. and Ripken, John F., Steady-State Cavity Studies in a Free-Jet Water Tunnel, University of Minnesota, St. Anthony Falls Hydraulic Laboratory, Project Report No. 47, July 1955.

[11] Johnson, Virgil E., Jr., Theoretical and Experimental Investigation of Supercavitating Hydrofoils Operating Near the Free Water Surface, National Aeronautics and Space Administration, Technical Report R-93, 1961.

[12] Silberman, E. and Song, C. S., "Instability of Ventilated Cavities," Journal of Ship Research, Vol. 5, No. 1, June 1961, pp. 13-33.

[13] Song, C. S., "Pulsation of Ventilated Cavities," Journal of Ship Research, Vol. 5, No. 4, March 1962, pp. 8-19.

[14] Hsu, C. C. and Chen, C. F., On the Pulsation of Finite, Ventilated Cavities, Hydronautics, Inc., Technical Report 115-4, November 1962.

F I G U R E S

(1 through 16)

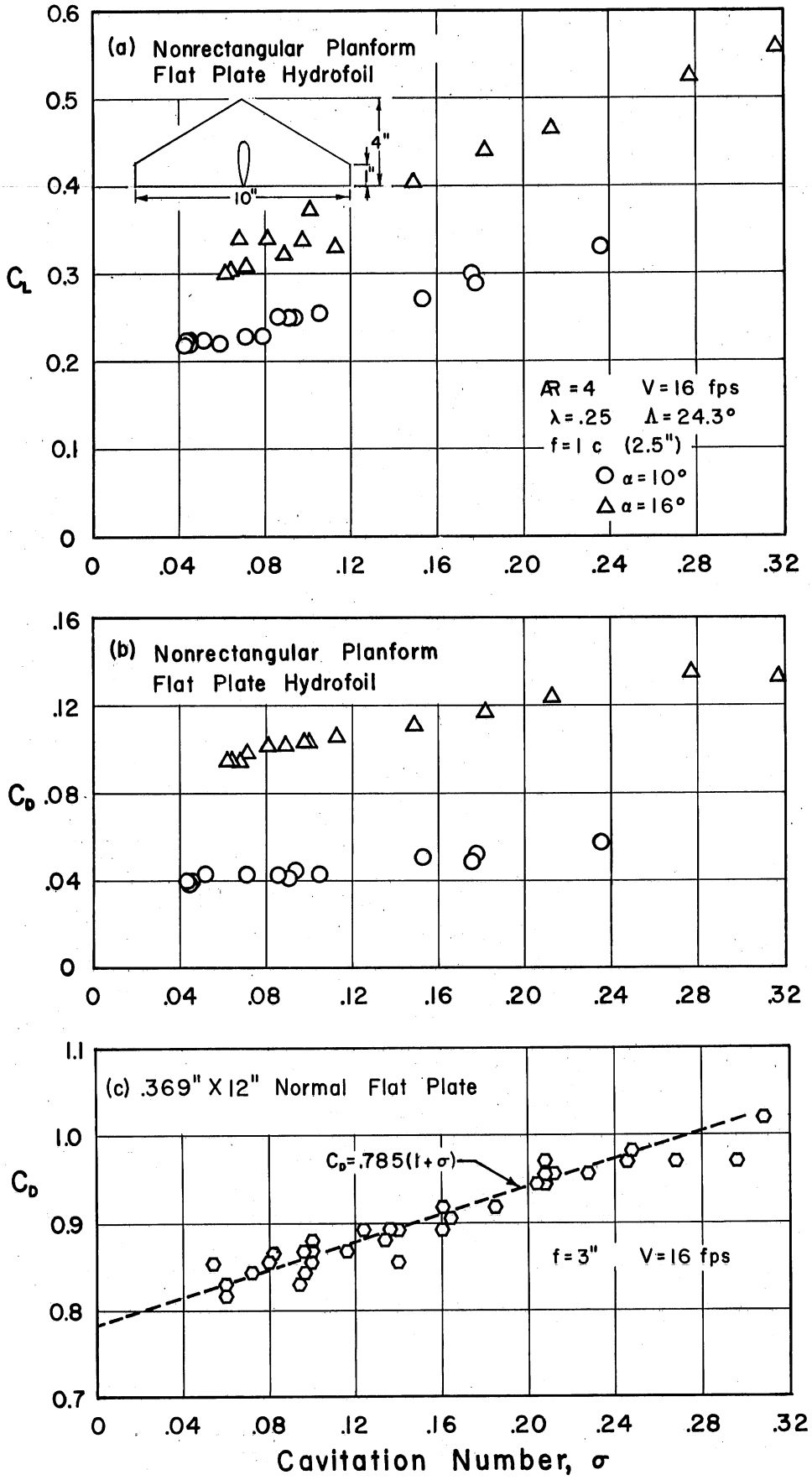

Fig. 1 - Force Coefficients for a Non-rectangular Planform Hydrofoil and a Normal Flat Plate

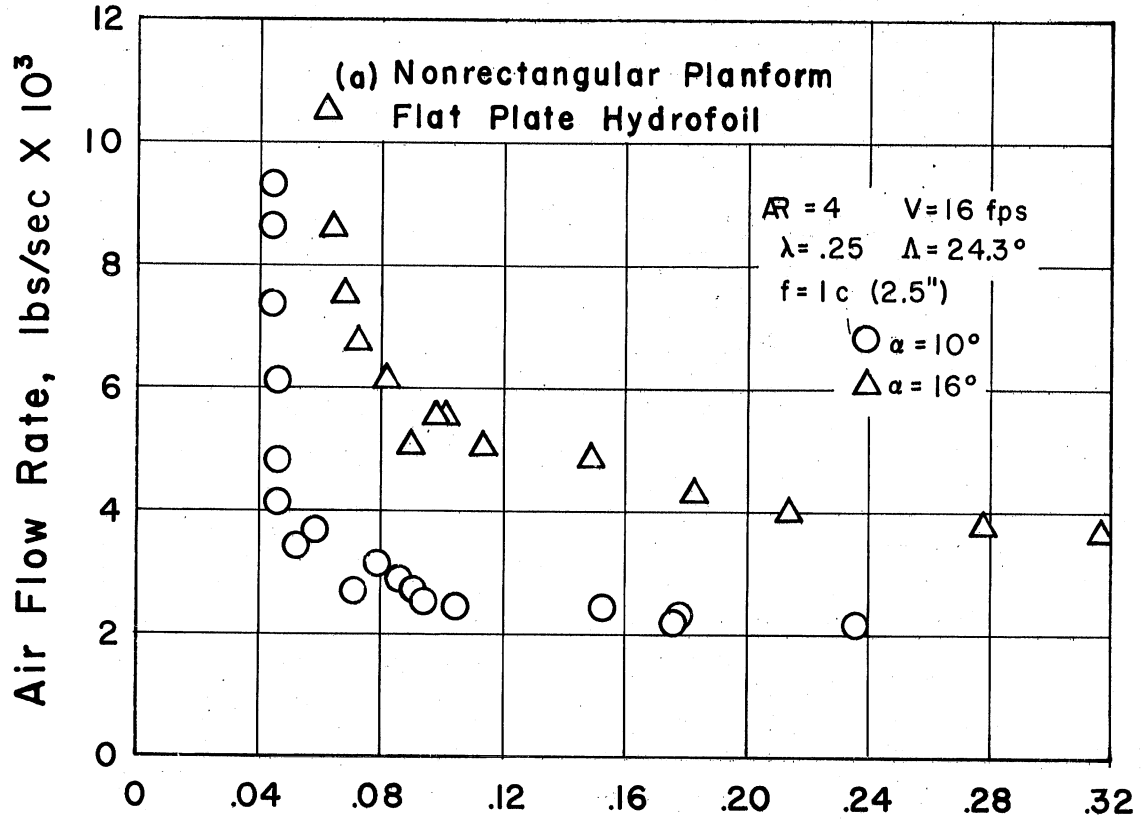

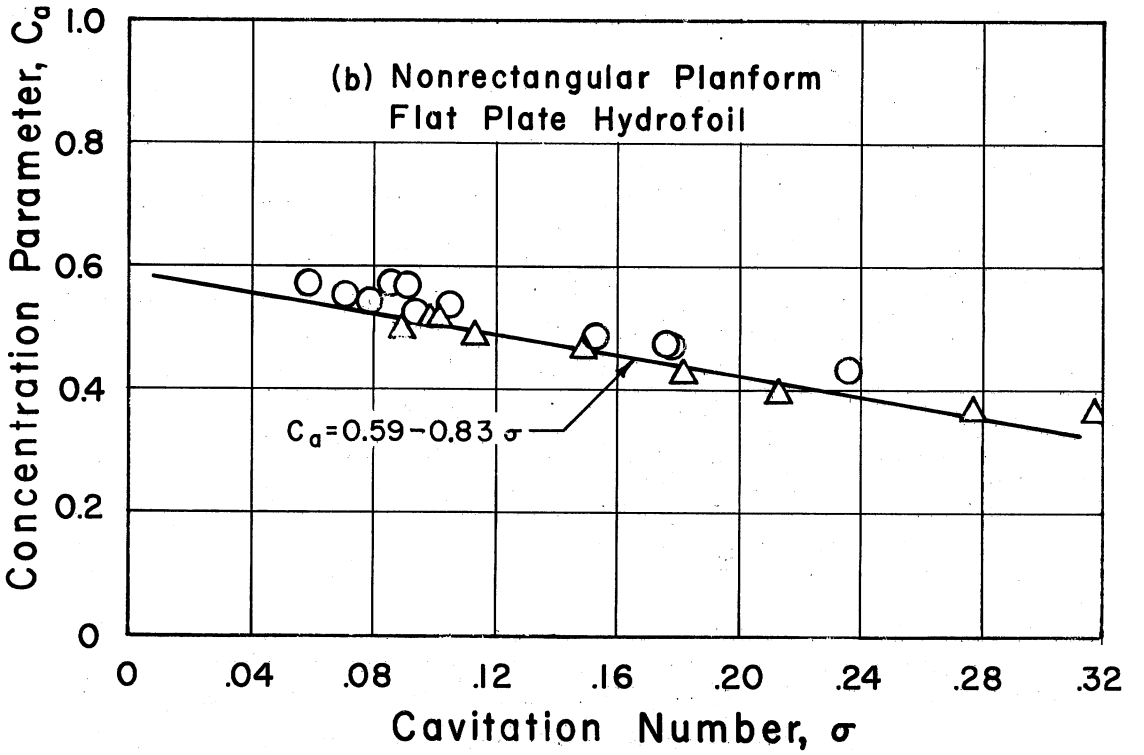

Fig. 2 - Air-entrainment Characteristics of Non-rectangular Planform Hydrofoil

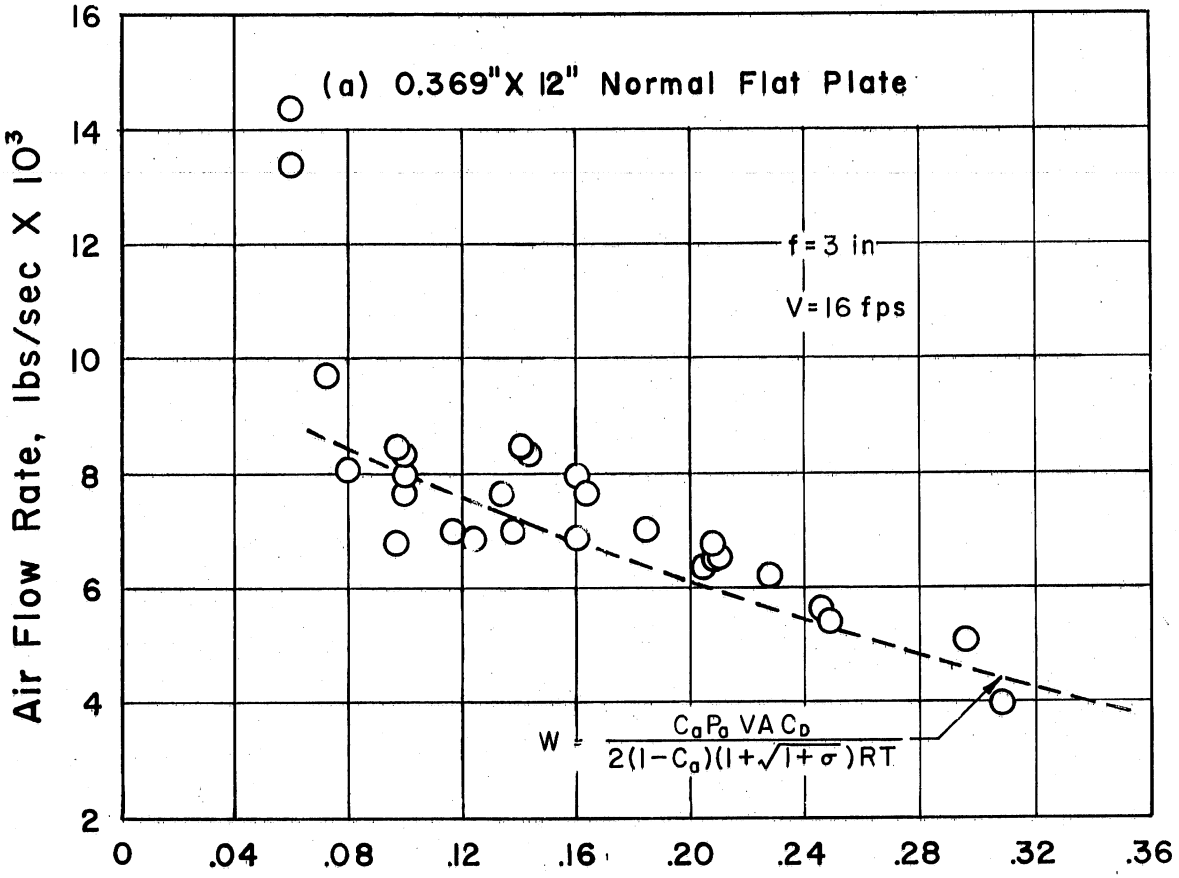

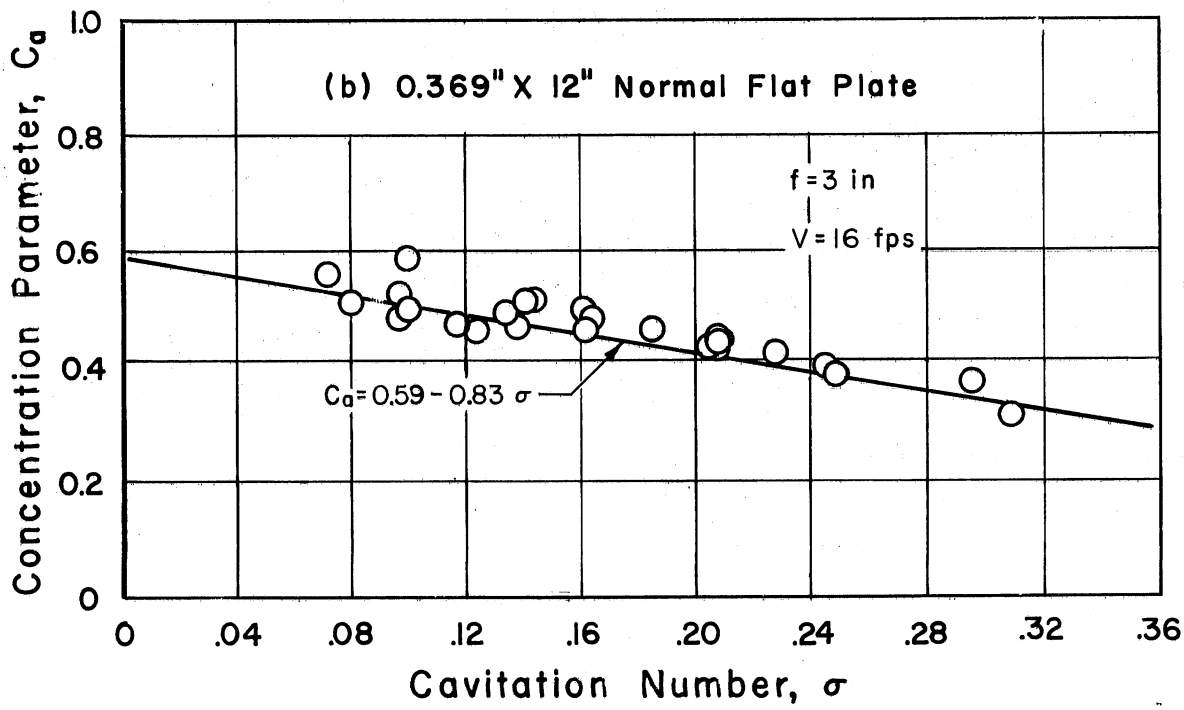

Fig. 3 - Air-entrainment Characteristics for a Flat Plate Normal to the Free Stream

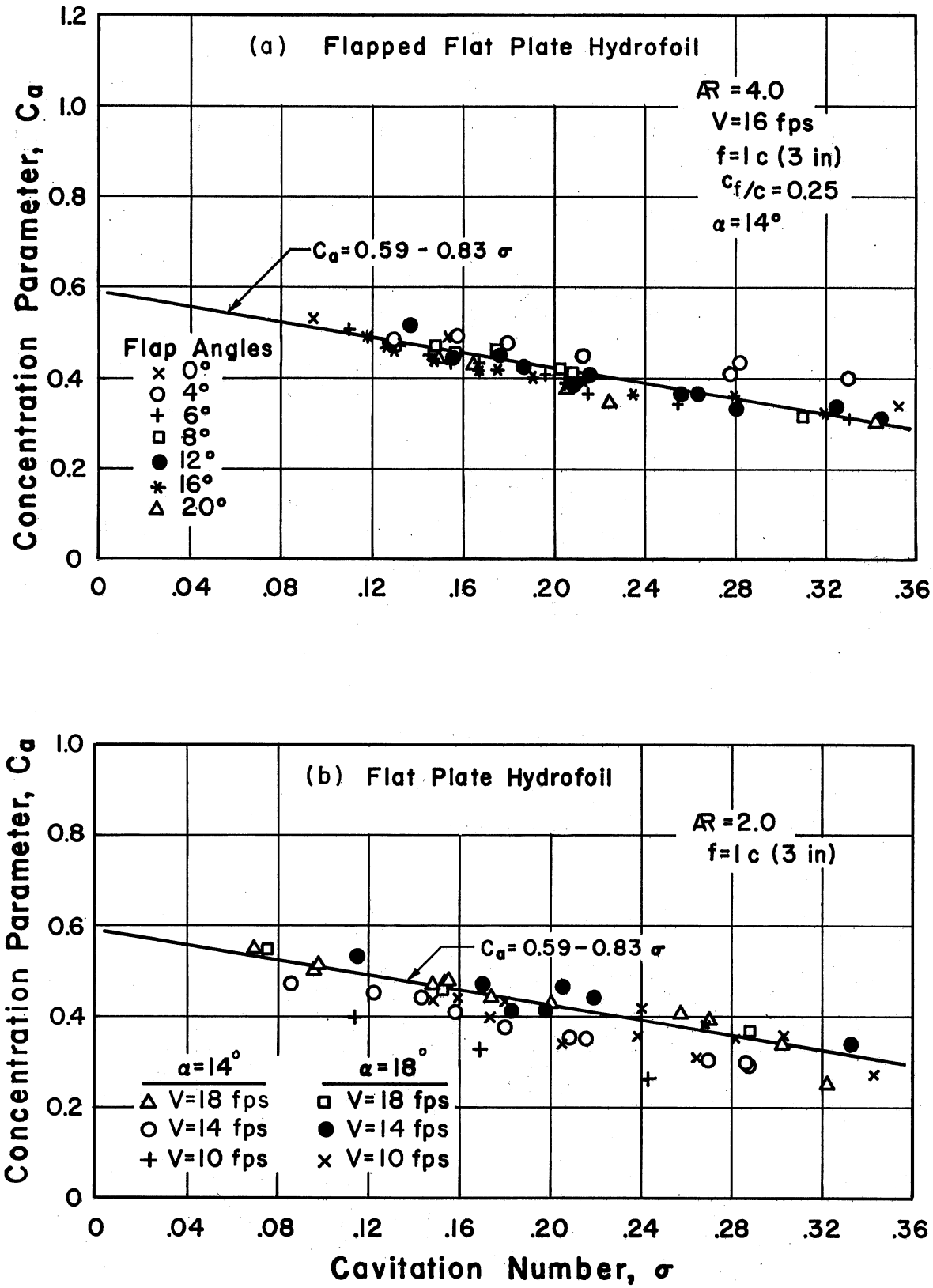

Fig. 4 - Air-entrainment Characteristics for Rectangular Planform Hydrofoils

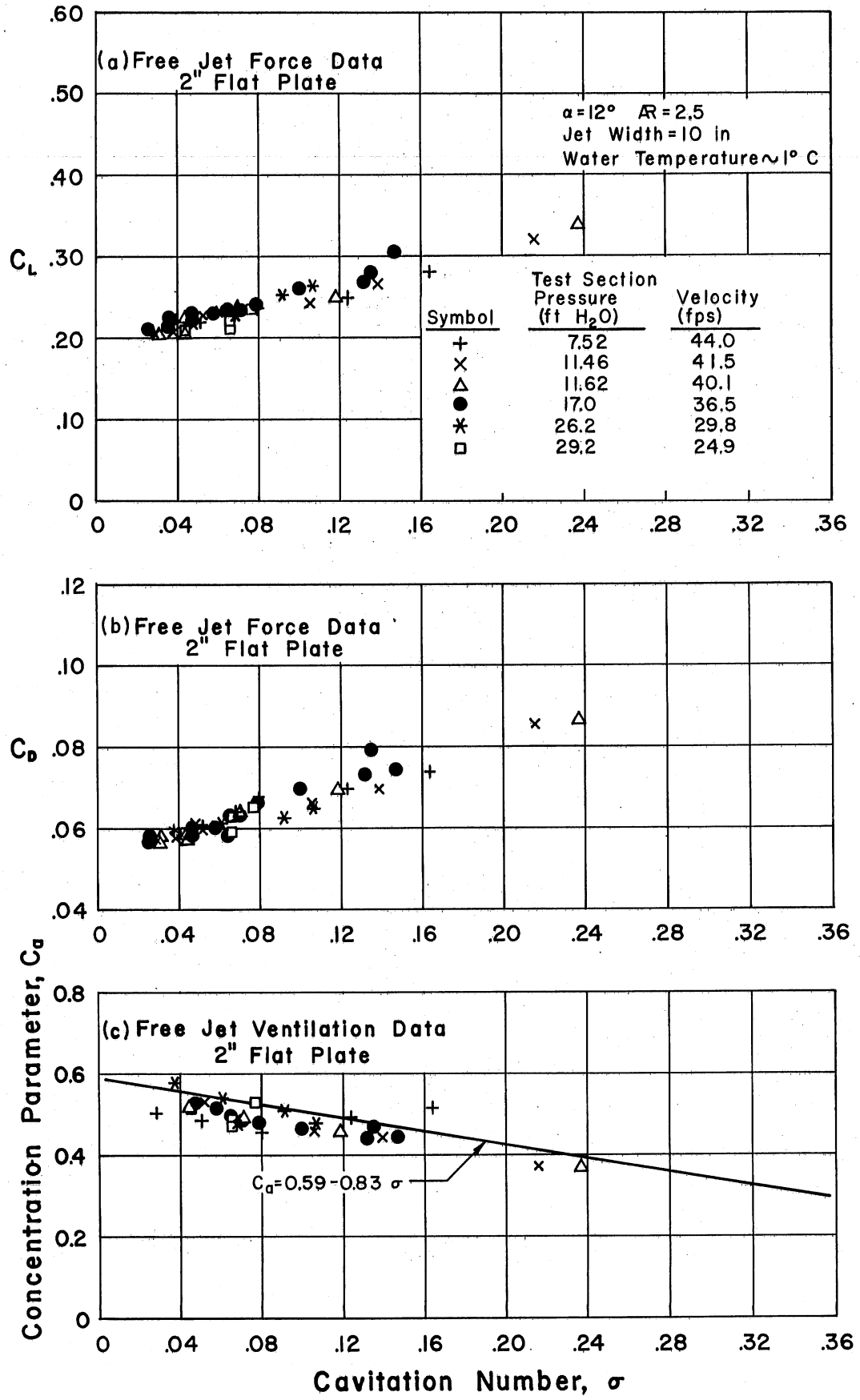

Fig. 5 - Force and Air-entrainment Characteristics for a Flat Plate in the Free Jet Water Tunnel

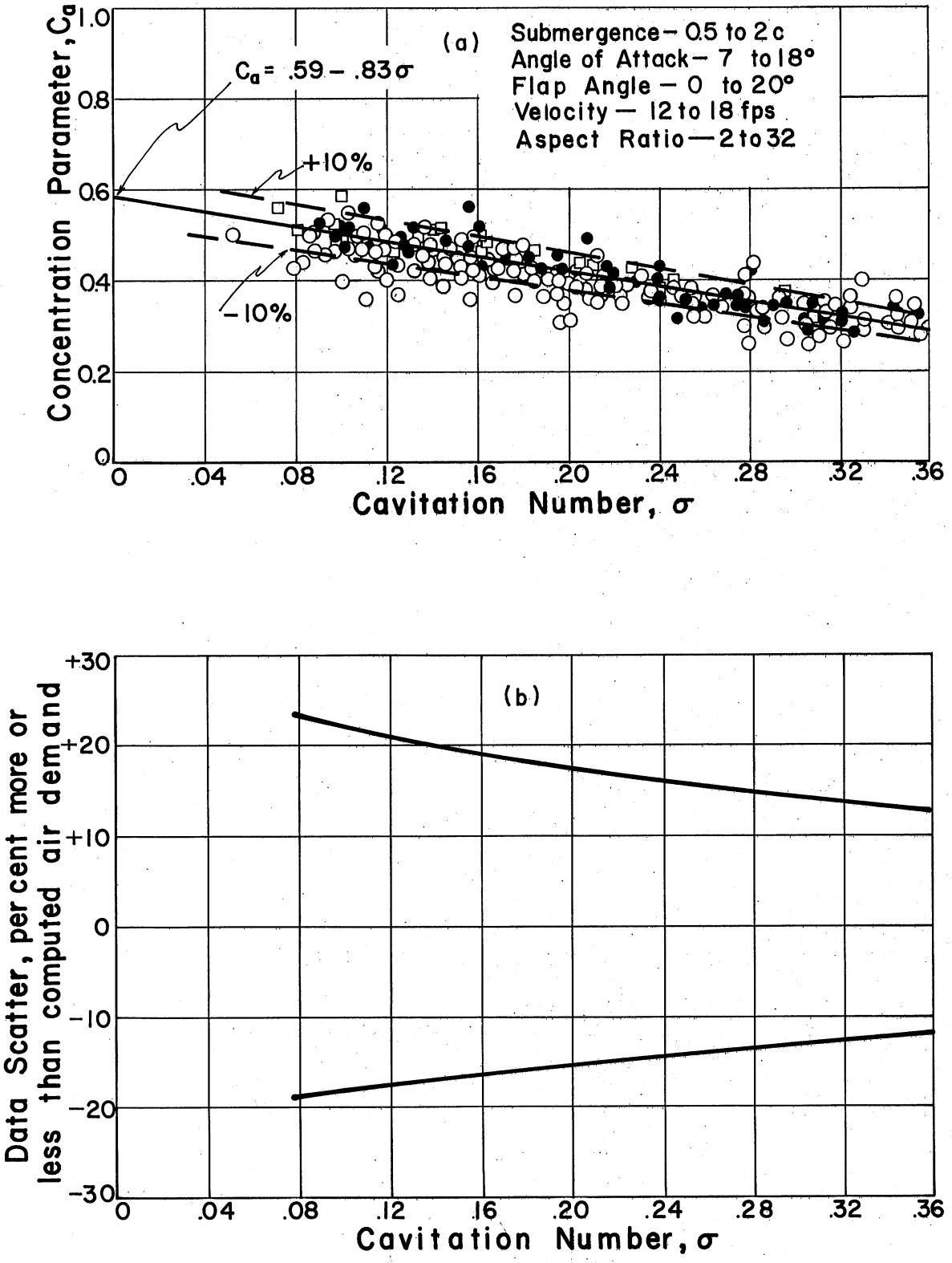

Fig. 6 – Summary of Air-entrainment Data Compared with Concentration Parameter

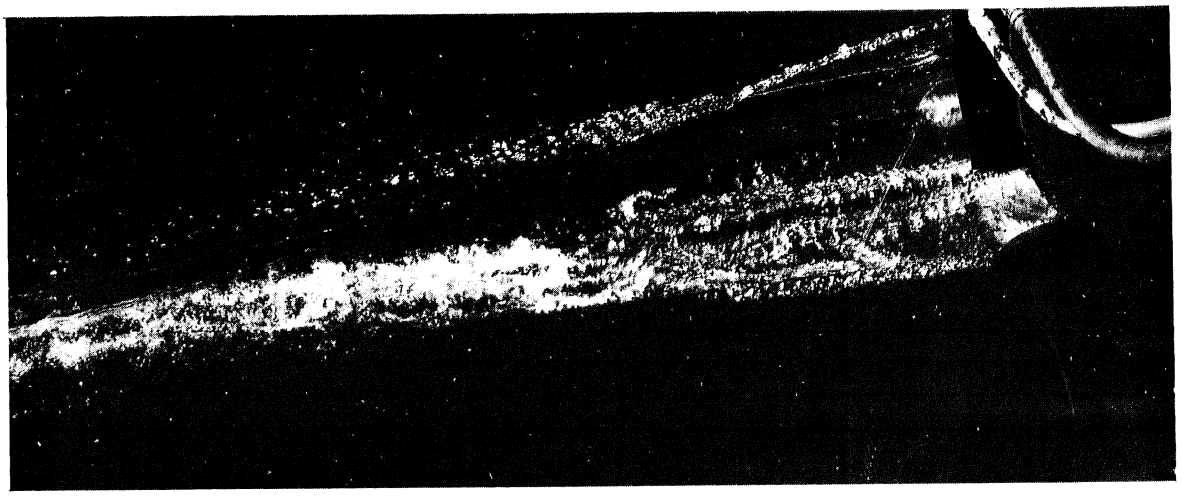

(a) 0.1 x 2° Tulin Profile , 3" Chord , AR = 3 , α = 17°

σ = .088 , V = 14 fps , f = 8"

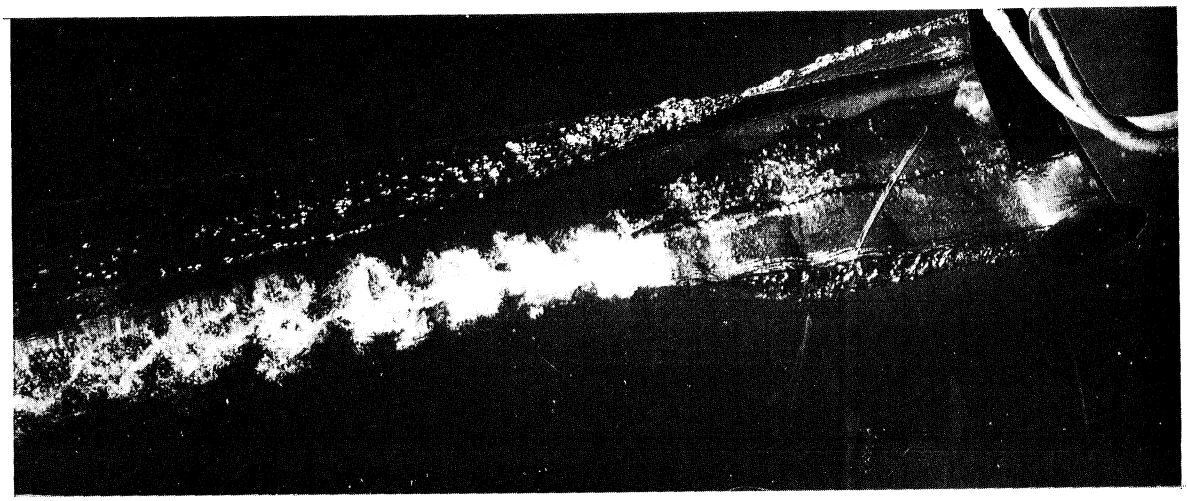

(b) 0.1 x 2° Tulin Profile , 3" Chord , AR = 3 , α = 17°

σ = .12 , V = 14 fps , f = 8"

Fig. 7 - Photographs of Cavities for a Cambered Foil with End Plates
(a) Trailing-vortex
(b) Pulsating

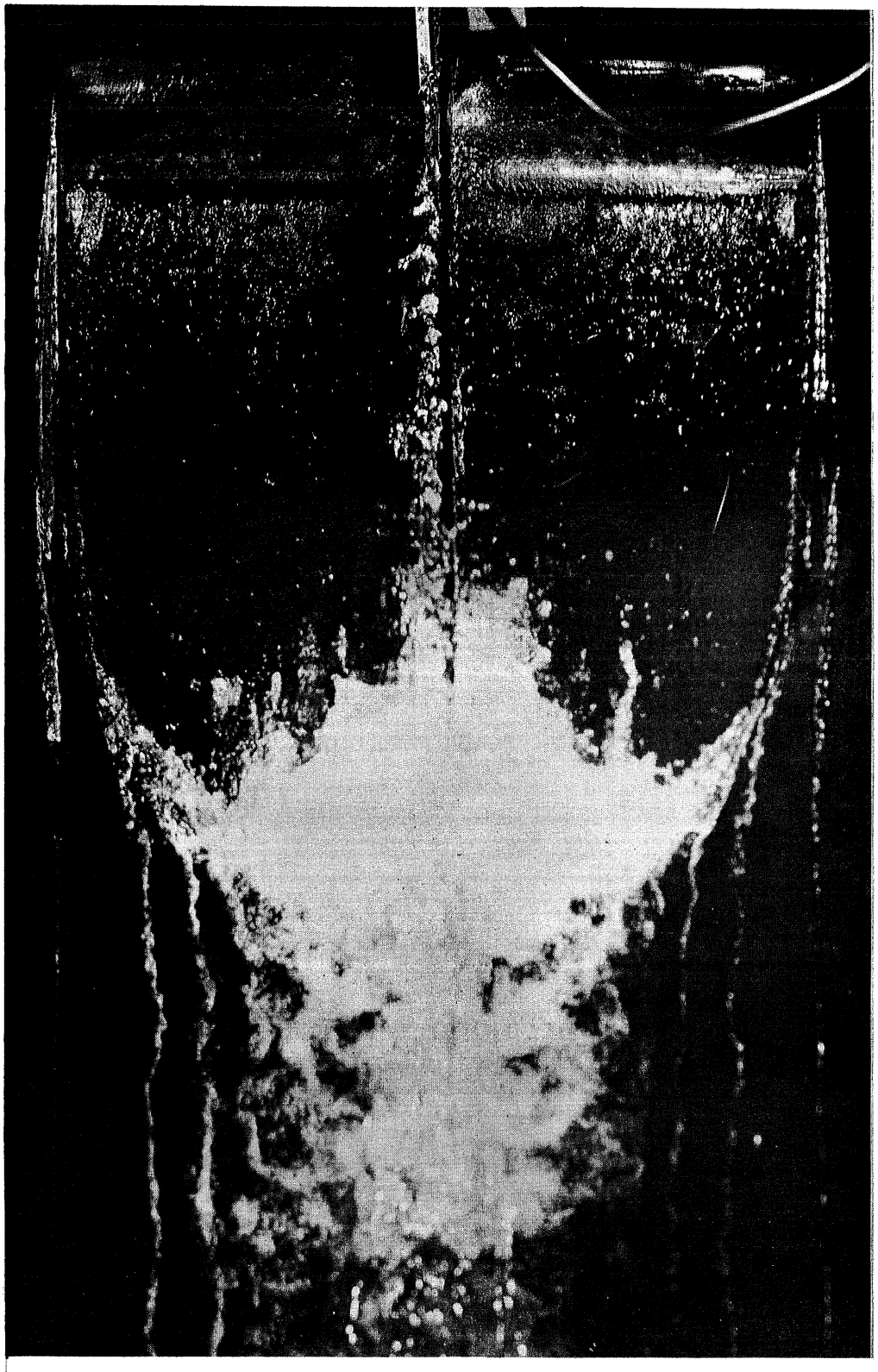

Fig. 8 - Multiple Pairs of Trailing Vortices on Cavity for Aspect Ratio 6 Flat Plate, $\alpha = 10^{\circ}$, f = 1 chord, $\sigma = 0.08$

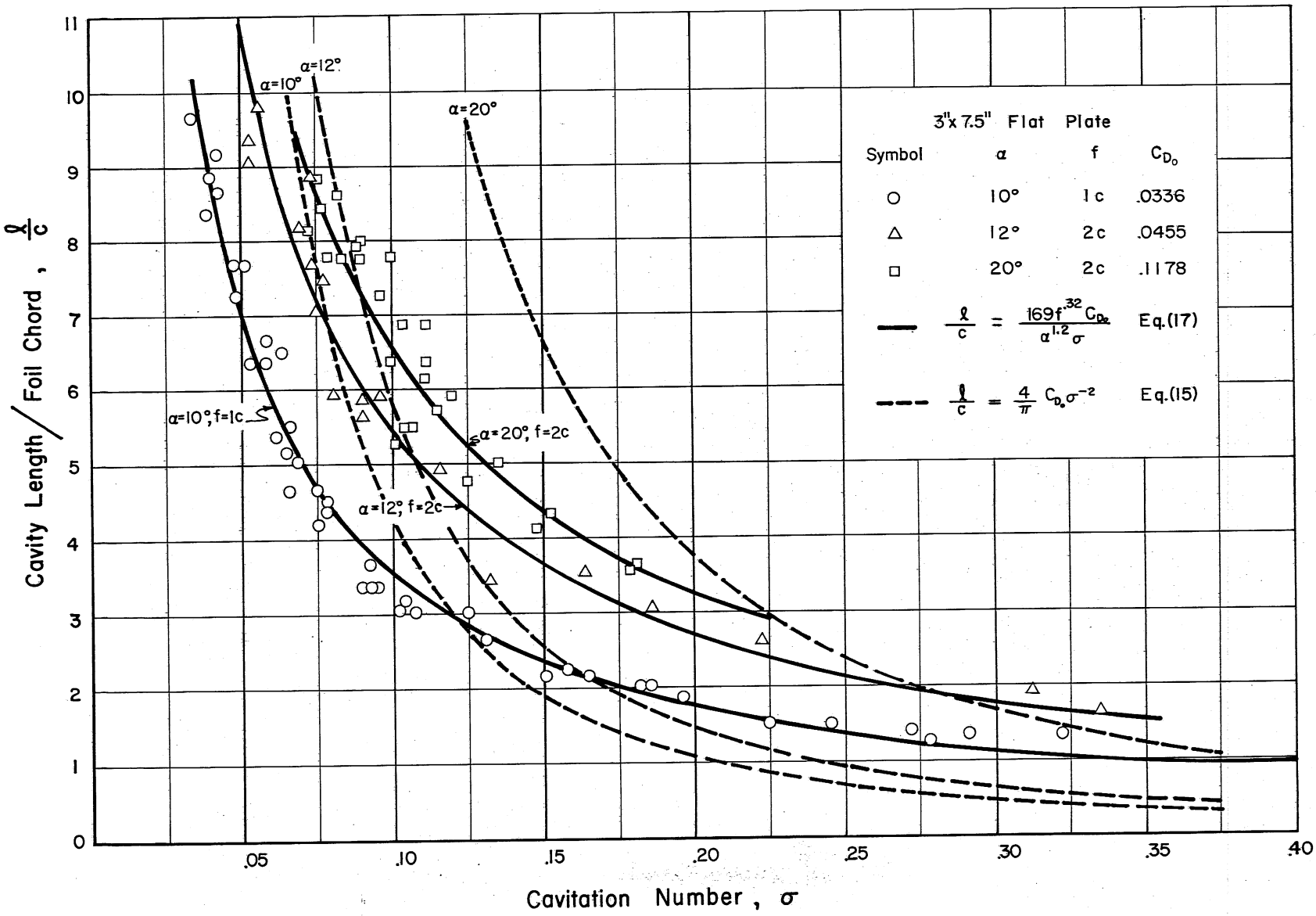

Fig. 9 - Typical Cavity Length Characteristics

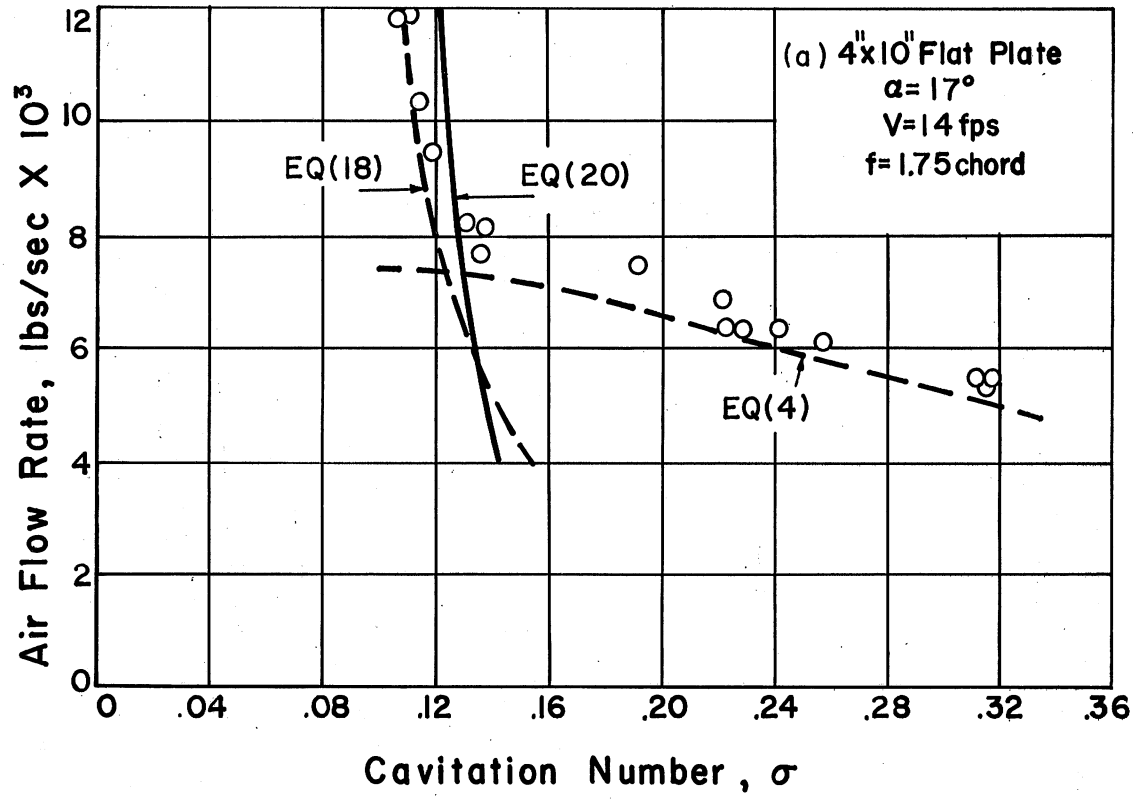

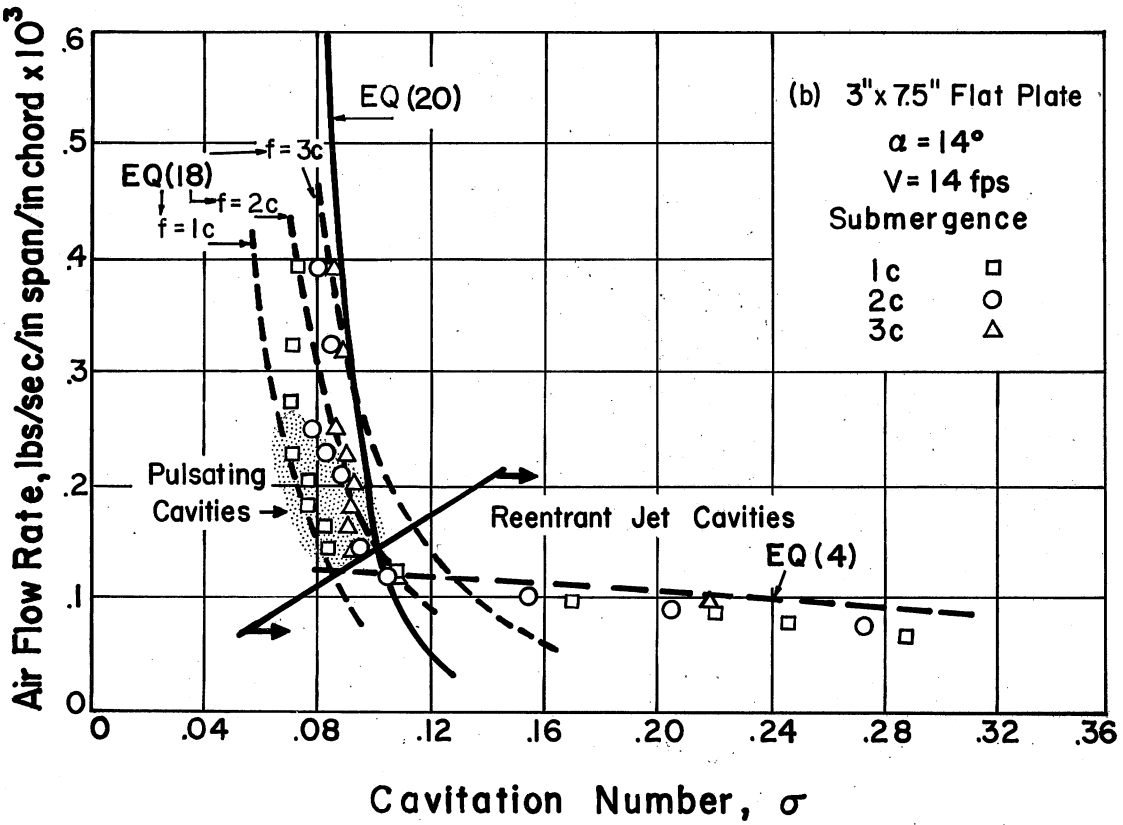

Fig. 10 - Comparison of Experimental and Calculated Air-entrainment Rates for Trailing Vortex and Reentrant Jet Cavities

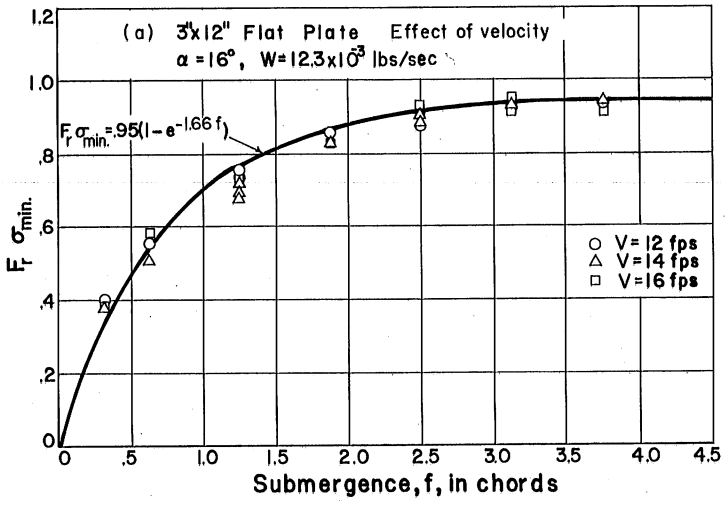

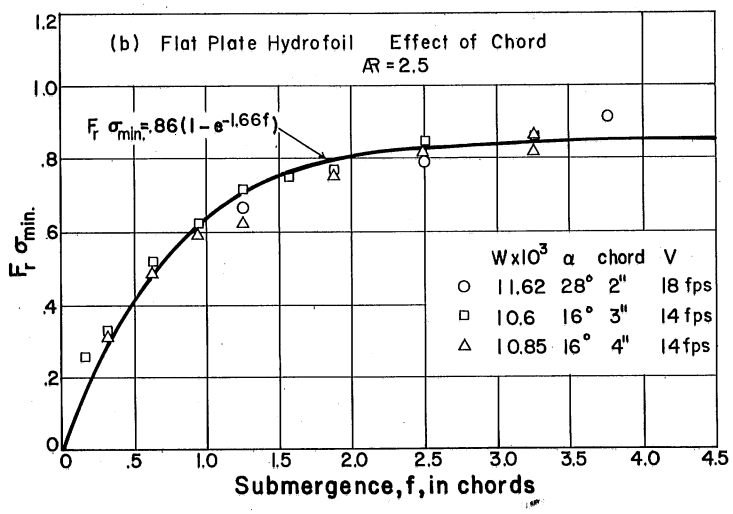

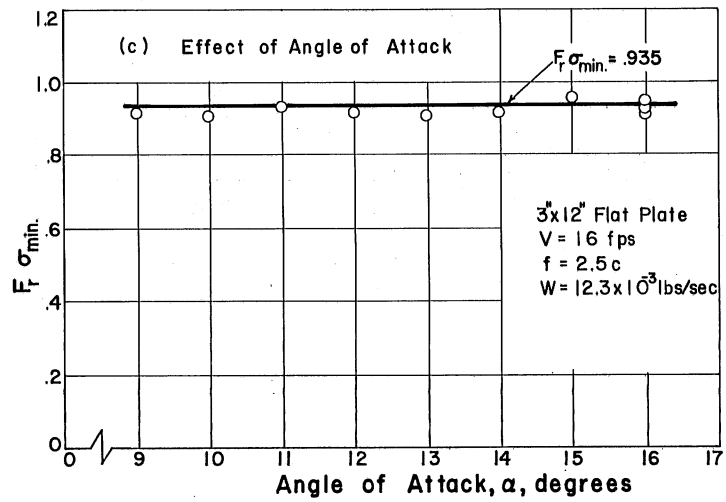

Fig. 11 - Effect of Submergence on Trailing Vortex Cavities

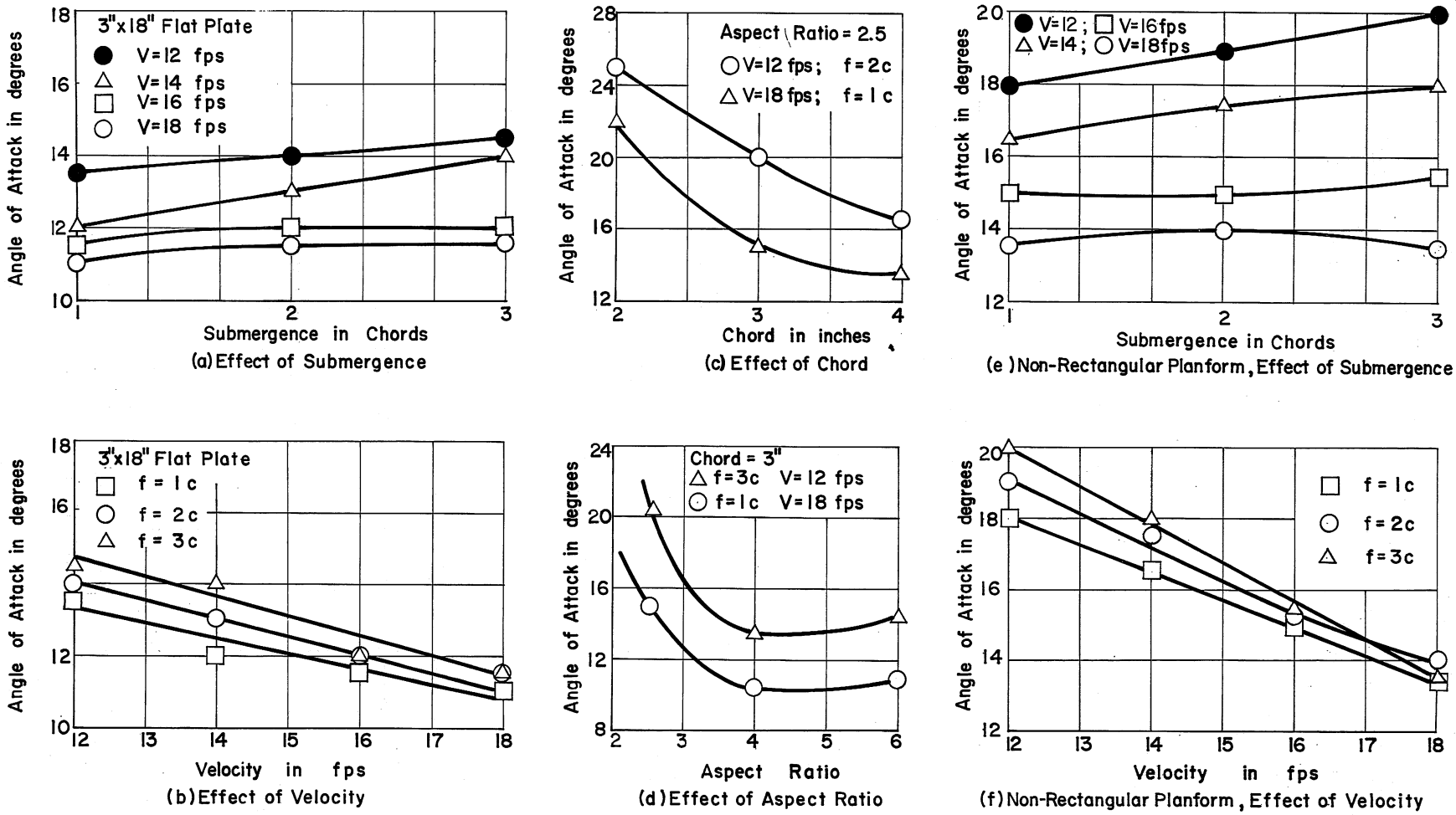

Above Curves — No Pulsation Below Curves — Pulsation

Fig. 12 - Stability Thresholds for Onset of Pulsation of Ventilated Cavities on Flat Plate Hydrofoils

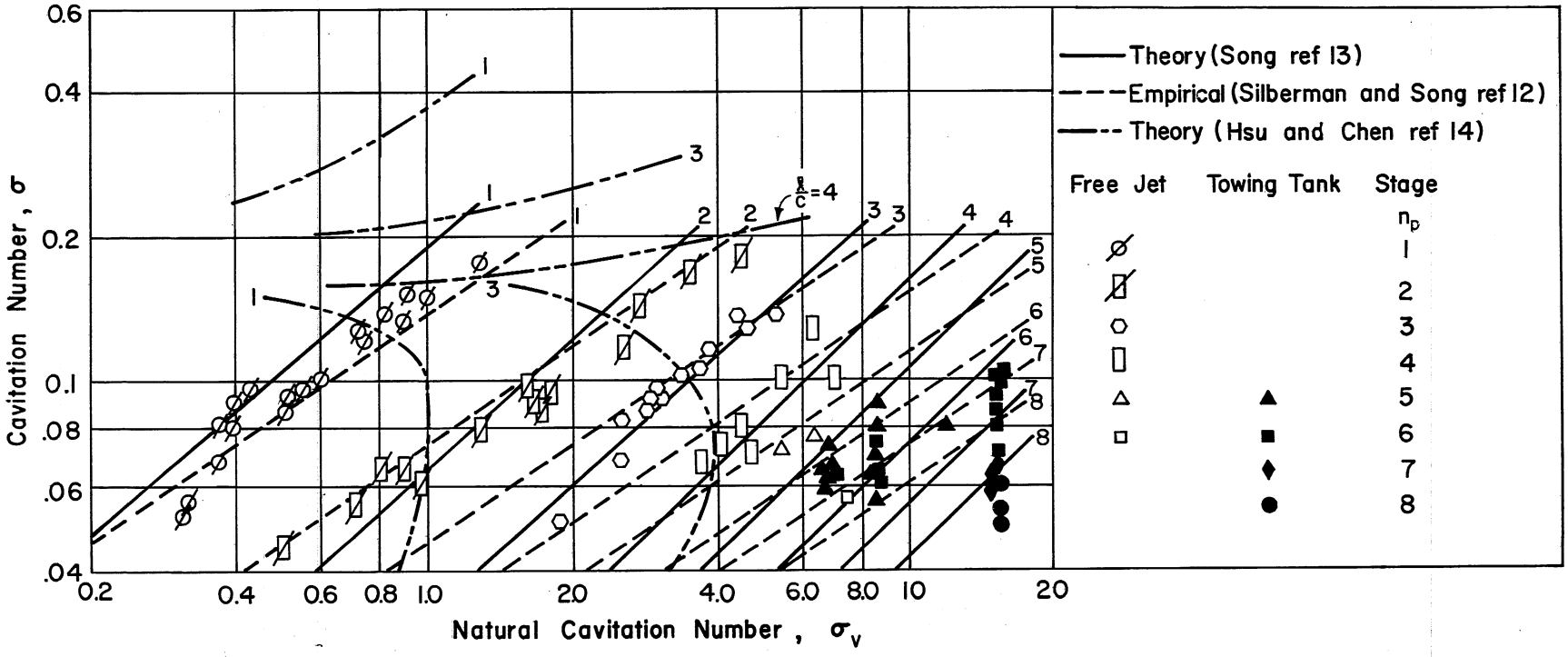

Fig. 13 - Comparison of Theory and Experimental Data for Pulsating Cavities

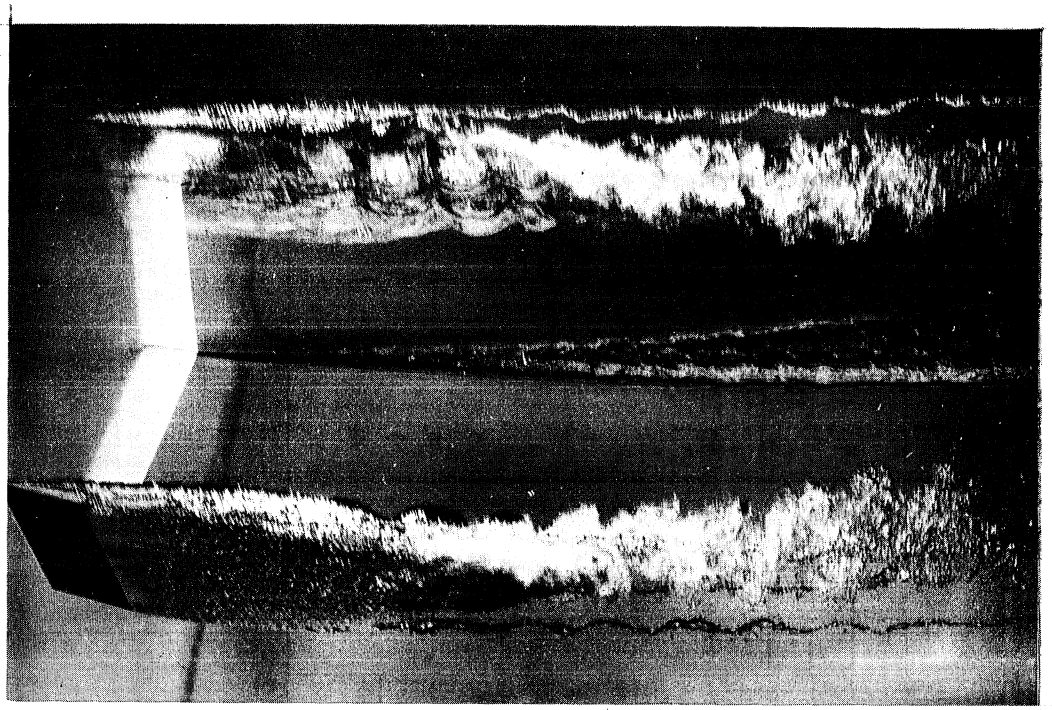

(a) $\alpha = +12°$, $f = 2.5\,c$, $W = 2.82 \times 10^{-3}$ lbs/sec
$\sigma = .101$, 3" Chord

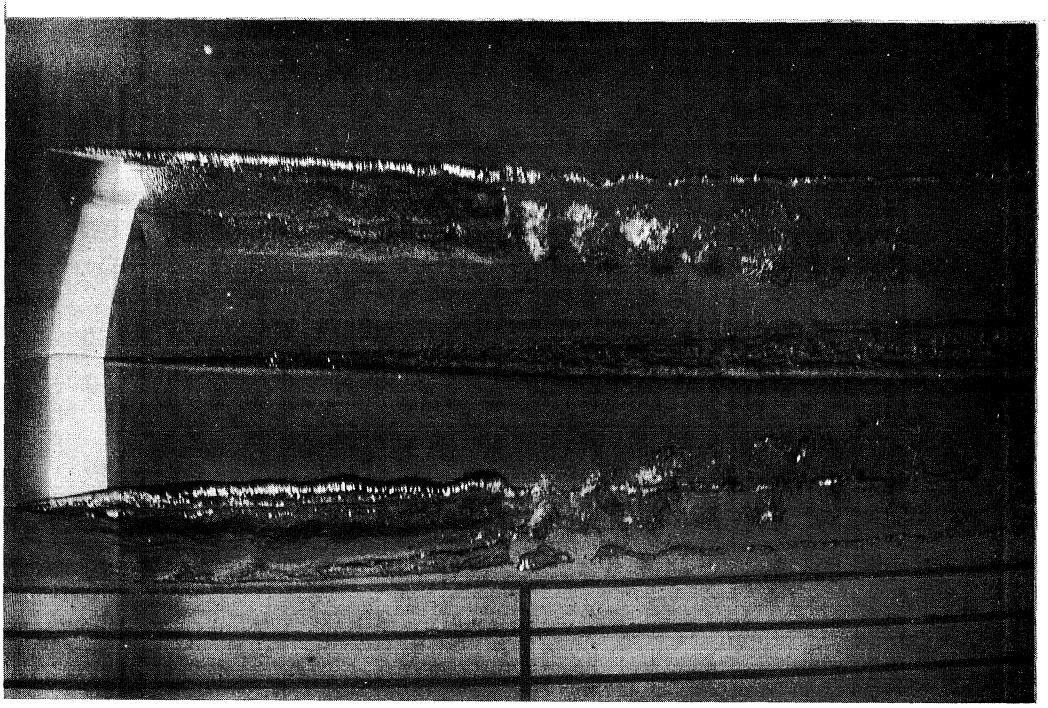

(b) $\alpha = -12°$, $f = 2.5\,c$, $W = 2.80 \times 10^{-3}$ lbs / sec
$\sigma \cong .080$, 3" Chord

Fig. 14 - Photographs of Cavity for Aspect Ratio 2.5 Foil at Positive and Negative Angles of Attack (Underwater View)

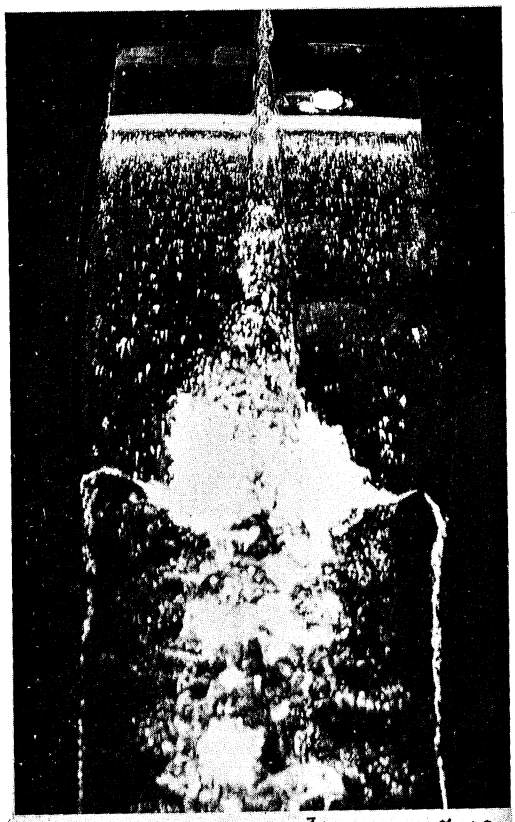

(a) $\alpha = -12°$, $W = 1.75 \times 10^{-3}$ lbs/sec, $\sigma \cong .10$

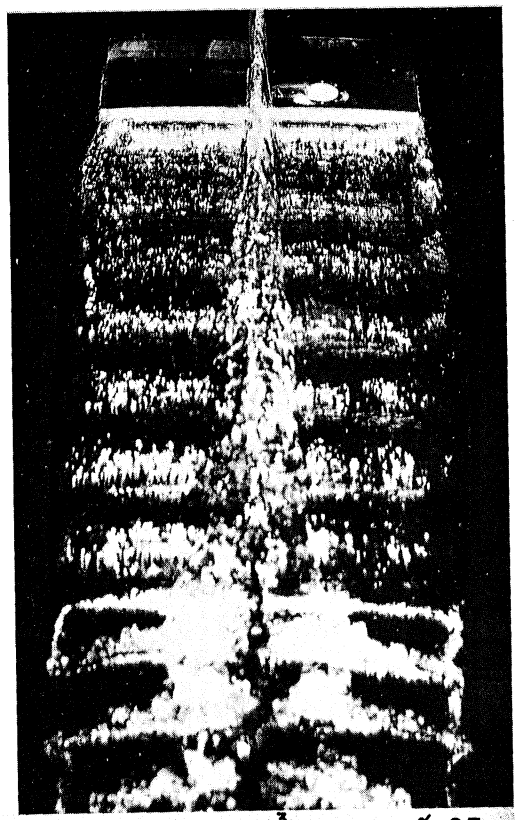

(b) $\alpha = -12°$, $W = 3.0 \times 10^{-3}$ lbs/sec, $\sigma \cong .07$

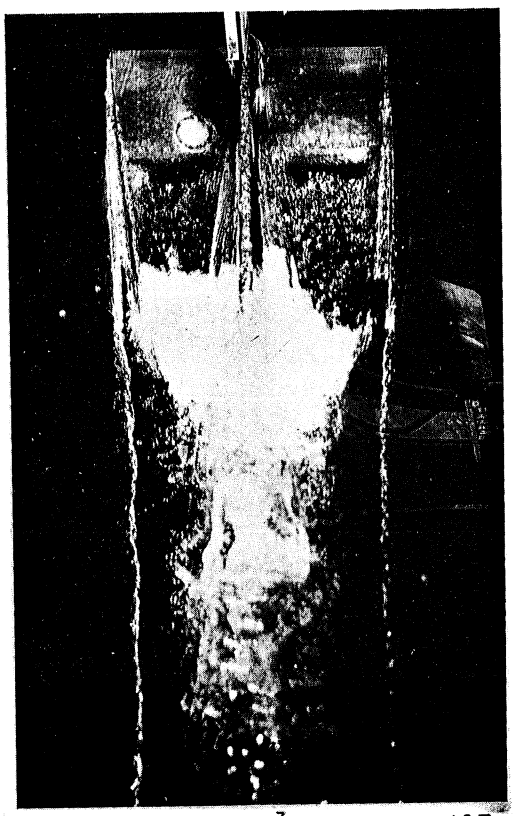

(c) $\alpha = +12°$, $W = 1.74 \times 10^{-3}$ lbs/sec, $\sigma = .107$

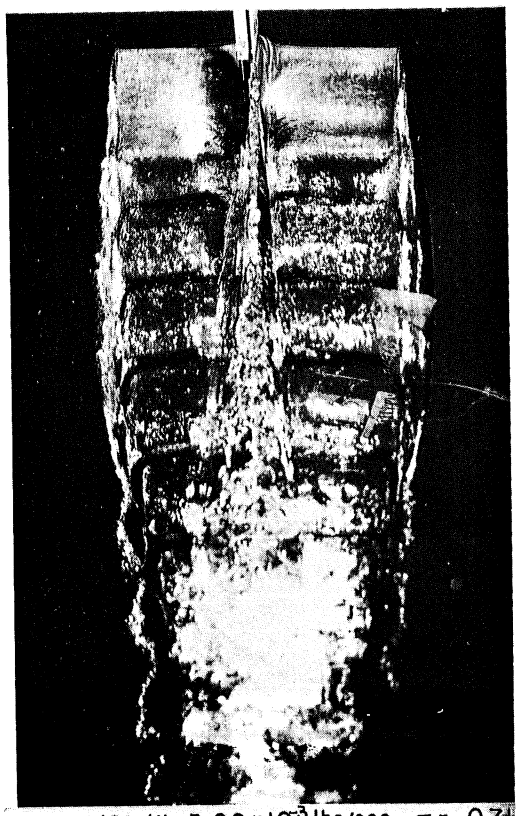

(d) $\alpha = +12°$, $W = 3.06 \times 10^{-3}$ lbs/sec, $\sigma = .071$

Fig. 15 - Photographs of Cavity for Aspect Ratio 2.5 Foil at Positive and Negative Angles of Attack (Plan View), V = 12 fps, f = 1c

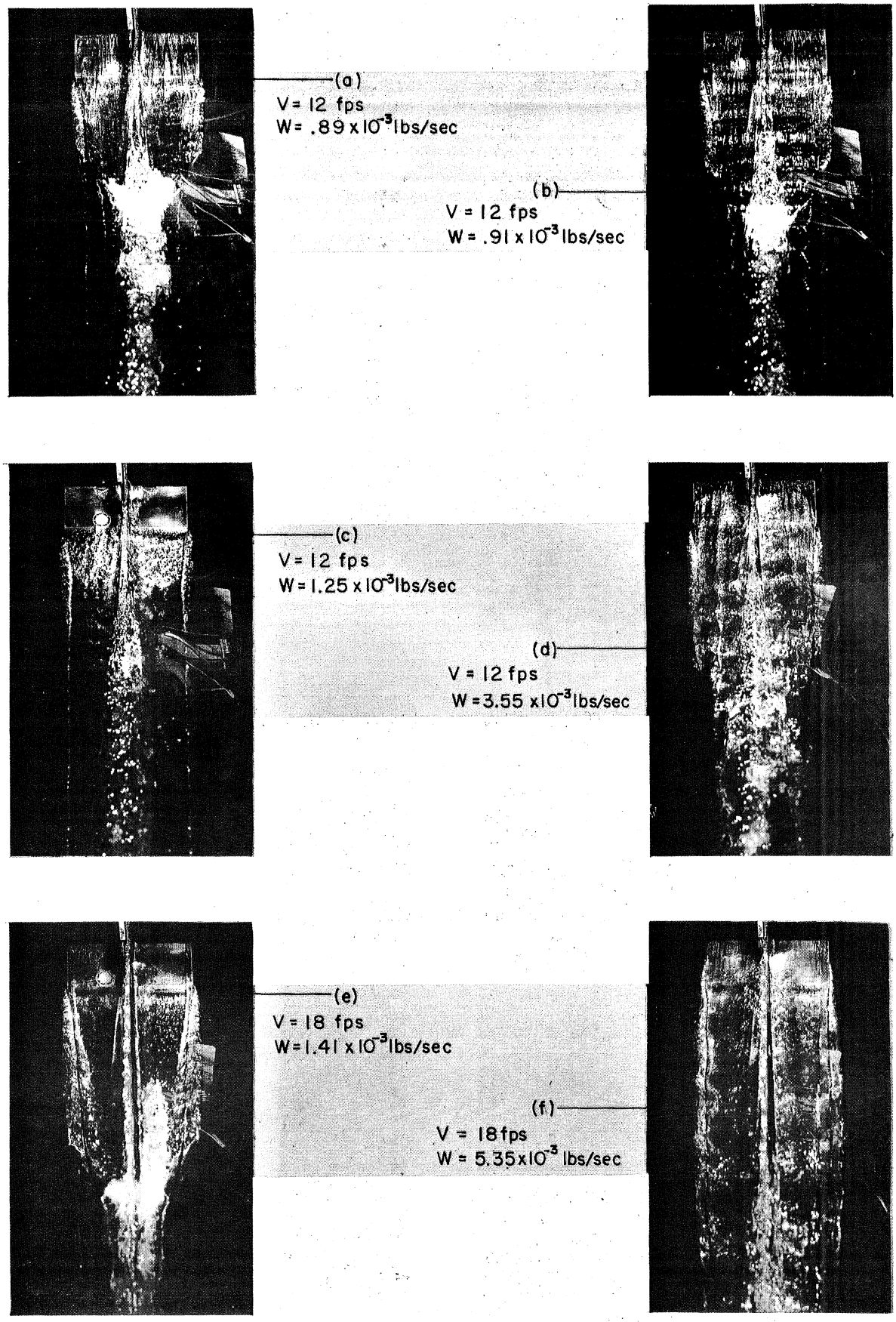

Fig. 16 - Photographs of Cavities on a Foil at 8 Degree Angle of Attack, $\alpha = 8^{\circ}$, f = 1c, AR = 2.5

A P P E N D I X

APPENDIX

The facilities utilized in the studies described in this report were the main towing tank and the free jet water tunnel in the St. Anthony Falls Hydraulic Laboratory.

The towing tank is 9 ft wide, 6 ft deep, and about 220 ft long. The water depth for all tests was maintained at 4.5 ft. A self-propelled carriage was used to obtain speeds up to 18 fps for these tests, the top speed being determined in this case by the time required to obtain a fully developed cavity and the available length of the channel for a test run.

The free jet water tunnel is a free-falling, nonrecirculating type utilizing Mississippi River water and with a transparent, vertical two-dimensional test section. The working velocity range of this tunnel is between 20 and 50 fps.

The majority of the bodies used in the experiments were flat foils with rectangular planforms. These are listed in the following table. The cross section of the hydrofoils was a 6 degree wedge with a hand-sharpened leading edge.

TABLE III

Chord, in.	Span, in.	Aspect Ratio
2	7.5	2.5
3	5	2.5
4	10	2.5
3	6	2
3	12	4
3	18	6

In addition to these hydrofoils, several other configurations were also tested. The 3- by 12-in. flat plate was fitted with fixed, full span flaps on the lower surface of the foil near the trailing edge. The ratio of the flap-chord to the foil-chord was 0.25 and the flap angles were 4, 6, 8, 12, 16, and 20 degrees. Also, a non-lifting flat plate with dimensions 0.369- by 12-in. was used. The small dimension was placed perpendicular to the free stream velocity. As most of the hydrofoils previously used in the investigation were of rectangular planform, it was of interest to conduct a series of tests with

a non-rectangular planform foil with a swept leading edge. This hydrofoil had a taper ratio λ of 0.25 with a 4-in. center chord, a 10-in. span, and an aspect ratio of 4 based on the mean chord of 2.5 inches. The trailing edge of the hydrofoil was not swept. This resulted in a sweepback angle, Λ, of the quarter chord line of 24.3 degrees. These foils are shown schematically in Fig. 1A.

Air was introduced into the cavity by ports at the base of the strut with a small supplementary supply to the leading edge in most cases. The ports at the base of the strut provided a stream of air that moved spanwise across the upper surface of the foil. The air jet issuing from the small tube to the leading edge was opposite to the direction of foil motion. This jet served as a means to ventilate a small separation bubble in that area as well as to stimulate a boundary layer separation at the lower angles of attack. Figure 1A shows a typical example of a hydrofoil constructed in this manner.

The strut in all cases was a NACA 0012 section with a 2-in. chord, attached to the foil at midspan. The location of the air ports with respect to the leading edge of the foil was not constant for all foils.

The cavity pressure was measured with a 1 psia Statham pressure transducer mounted directly on the strut above the water surface. A hypodermic tube running along the strut connected the transducer with a chamber machined into the suction face of the foil and located aft of the midchord. A very thin plastic diaphragm was loosely placed over the chamber. The entire system then was filled with hydraulic oil. This type of pressure-measurement system permitted a continuous record of the cavity pressure during the test run, although it was not suitable for measuring pressure fluctuations because of its inherent high damping and low frequency response characteristics.

In a limited series of tests, a 2-1/2 psia Statham miniature pressure transducer was mounted directly on a 4-in. by 10-in. foil with its diaphragm exposed to the interior of the cavity. This arrangement was used in pilot studies of a limited nature to detect transient and unsteady cavity behavior such as the amplitude of the pressure fluctuations associated with pulsating cavities.

The air-flow rate was measured with an orifice meter placed in the supply line. Several auxiliary air tanks on the carriage were used for the air supply. An essentially constant upstream pressure was maintained by means of a pressure

reducer placed in the line between the air tanks and the orifice meter. Pressures and temperatures were recorded to permit determination of the air-flow rate.

The foil strut was attached to a device that permitted adjustment of the angle of attack within 1/4 degree and a dynamometer for measuring lift and drag forces for the various cavity conditions. The unit was attached to a towing strut with which the submergence could be varied. The dynamometer was of the two-component strain-gage type in which the lift and drag could be recorded independently, simultaneously, and continuously during the test.

The force and pressure signals were recorded on a Sanborn four-channel recorder mounted on the carriage. A record of the instantaneous carriage speed was also obtained. This permitted a direct determination of the length of test run, which was extremely useful in evaluating the significance of transient effects of the cavity associated with the acceleration of the carriage.

The foil was set at a given angle of attack and submergence. The angle of attack was measured from the chord line and the submergence was measured from the water surface to the leading edge of the foil in all cases, as shown in Fig. 1A. The chord, c, was taken as the distance from leading to trailing edge. The Reynolds number based on chord length of the plate varied from 1×10^5 to 6×10^5 at an essentially constant water temperature of 17° C. A range of submergences from about 0.25 to 3.75 chords was selected, although all submergences were not used for each profile. Runs were first made for a particular angle of attack and submergence with no air admitted to the foil to determine the extent of natural ventilation, if any. For all tests reported, no cavitation or ventilation of any type was observed until the metered air was supplied in the region of the foil. Also, only cases where supercavitation occurred (cavity covering the entire chord or more of the foil) are reported.

Before each run, the air-flow rate was adjusted to a predetermined value. After the carriage acceleration period and after a full cavity across the span was formed, the flow rate was again checked. The cavity pressure and forces were continuously recorded with the Sanborn recorder. Photographs of the cavity were then taken with a 200 μ sec electronic flash for a number of conditions and were used to determine cavity lengths. A reference mark was made on the Sanborn record at the instant the photo was taken. A stroboscopic light was used to visually determine the extent of cavity pulsation as evidenced by the formation of waves on the surface of the cavity.

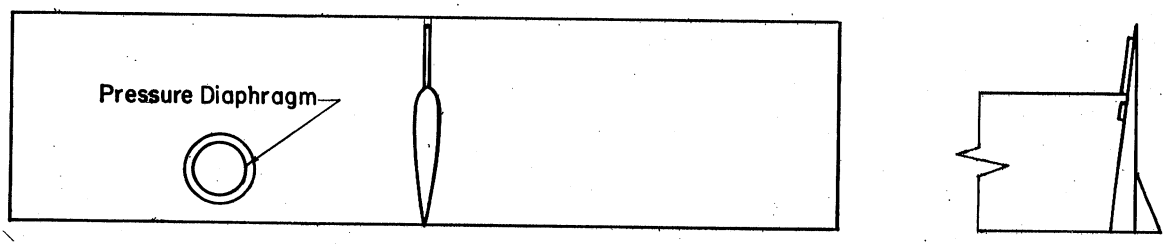

(a) Flapped Hydrofoil

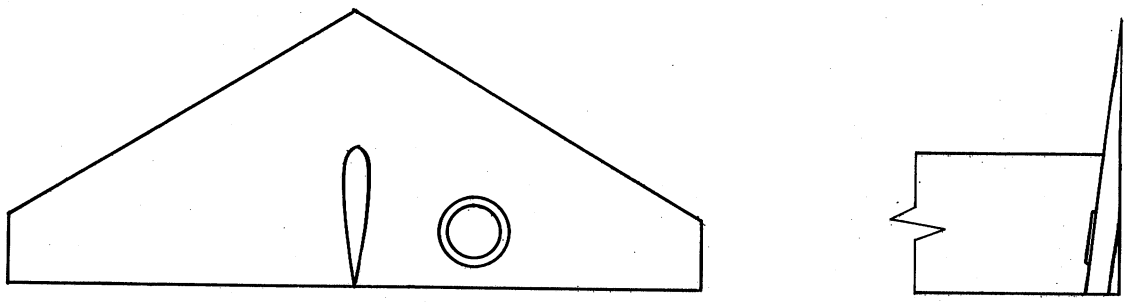

(b) Tapered Hydrofoil

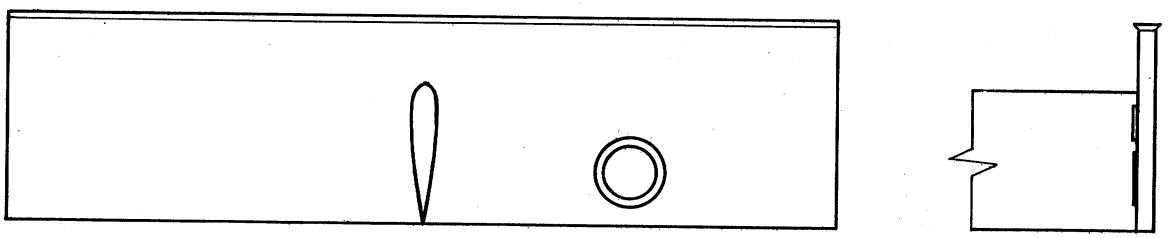

(c) Non-lifting Flat Plate

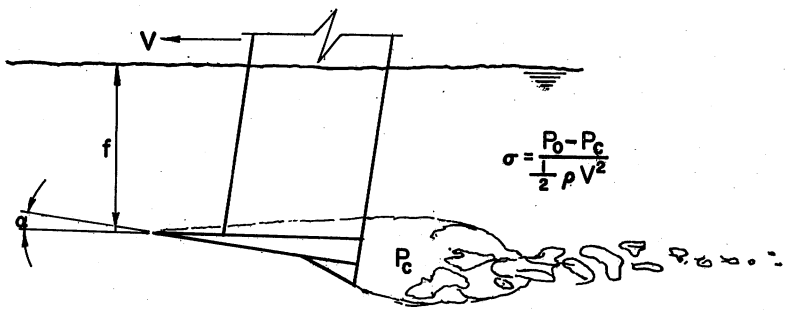

(d) Flow Conditions

Fig. 1A - Definition Sketch

DISTRIBUTION LIST FOR PROJECT REPORT NO. 72

of the St. Anthony Falls Hydraulic Laboratory

Copies	Organization
6	Chief of Naval Research, Department of the Navy, Washington, D. C. 20360, Attn: 3 - Code 438 1 - Code 461 1 - Code 463 1 - Code 466
1	Commanding Officer, Office of Naval Research, Branch Office, 495 Summer Street, Boston 10, Massachusetts.
1	Commanding Officer, Office of Naval Research, Branch Office, 219 S. Dearborn St., Chicago, Illinois 60604
1	Commanding Officer, Office of Naval Research, Branch Office, 207 West 24th Street, New York 11, New York.
25	Commanding Officer, Office of Naval Research, Branch Office, Navy No. 100, Box 39, Fleet Post Office, New York, New York.
1	Commanding Officer, Office of Naval Research, Branch Office, 1030 East Green Street, Pasadena 1, California.
1	Commanding Officer, Office of Naval Research, Branch Office, 1000 Geary Street, San Francisco 9, California.
1	Director, Naval Research Laboratory, Washington 25, D. C., Attn: Code 2027.
3	Chief, Bureau of Naval Weapons, Department of the Navy, Washington 25, D. C., Attn: 1 - Code RRRE 1 - Code RAAD 1 - Code RAAD-222
7	Chief, Bureau of Ships, Department of the Navy, Washington 25, D. C. Attn: 1 - Code 312 1 - Code 335 1 - Code 420 1 - Code 421 1 - Code 440 1 - Code 442 1 - Code 449
1	Chief, Bureau of Yards and Docks, Department of the Navy, Washington 25, D. C. Attn: Code D-400.
12	Commanding Officer and Director, David Taylor Model Basin, Washington 7, D. C., Attn: 1 - Code 500 1 - Code 513

Copies	Organization
	1 - Code 520 1 - Code 525 1 - Code 526 1 - Code 526A 1 - Code 530 1 - Code 533 1 - Code 580 1 - Code 585 1 - Code 589 1 - Code 700
1	Commander, Naval Ordnance Test Station, China Lake, California, Attn: Code 753.
1	Commander, Naval Ordnance Test Station, Pasadena Annex, 3202 E. Foothill Boulevard, Pasadena 8, California, Attn: Code P508.
1	Commander, Portsmouth Naval Shipyard, Portsmouth, New Hampshire, Attn: Planning Department.
1	Commander, Boston Naval Shipyard, Boston, Massachusetts, Attn: Planning Department.
1	Commander, Pearl Harbor Naval Shipyard, Navy No. 128, Fleet Post Office, San Francisco, California, Attn: Planning Department.
1	Commander, San Francisco Naval Shipyard, San Francisco, California, Attn: Planning Department.
1	Commander, Mare Island Naval Shipyard, Vallejo, California, Attn: Planning Department.
1	Commander, New York Naval Shipyard, Brooklyn 1, New York, Attn: Planning Department.
1	Commander, Puget Sound Naval Shipyard, Bremerton, Washington, Attn: Planning Department.
1	Commander, Philadelphia Naval Shipyard, Philadelphia, Pennsylvania, Attn: Planning Department.
1	Commander, Norfolk Naval Shipyard, Portsmouth, Virginia, Attn: Planning Department.
1	Commander, Charleston Naval Shipyard, Charleston, South Carolina, Attn: Planning Department.
1	Commander, Long Beach Naval Shipyard, Long Beach 2, California, Attn: Planning Department.
1	Commander, US Naval Weapons Laboratory, Dahlgren, Virginia, Attn: Planning Department.
1	Commander, US Naval Ordnance Laboratory, White Oak, Maryland.
1	Commander, US Naval Weapons Laboratory, Dahlgren, Virginia, Attn: Computation and Exterior Ballistics Laboratory (Dr. A. V. Hershey).
1	Superintendent, US Naval Academy, Annapolis, Maryland, Attn: Library.

Copies	Organization
1	Superintendent, US Naval Postgraduate School, Monterey, California.
1	Commandant, US Coast Guard, 1300 E Street, NW, Washington, D. C.
1	Secretary, Ship Structure Committee, US Coast Guard Headquarters, 1300 E Street, NW, Washington, D. C.
1	Commander, Military Sea Transportation Service, Department of the Navy, Washington 25, D. C.
1	Division of Ship Design, Maritime Administration, 441 G Street, NW, Washington 25, D. C.
1	Superintendent, US Merchant Marine Academy, Kings Point, Long Island, New York, Attn: Captain L. S. McCready.
1	Commanding Officer and Director, US Navy Mine Defense Laboratory, Panama City, Florida.
1	Commanding Officer, NROTC and Naval Administrative Unit, Massachusetts Institute of Technology, Cambridge 39, Massachusetts.
1	Commander, Hdqs. US Army Transportation Research and Development Command, Transportation Corps, Fort Eustis, Virginia, Attn: Marine Transportation Division.
1	Air Force Office of Scientific Research, Mechanics Division, Washington 25, D. C.
1	Commander, Wright Air Development Division, Aircraft Laboratory, Wright-Patterson Air Force Base, Ohio, Attn: Mr. W. Mykytow, Dynamics Branch.
1	Director of Research, Code RR, National Aeronautics and Space Administration, 600 Independence Avenue, SW, Washington, D. C. 20546.
1	Director, Langley Research Center, Langley Station, Hampton, Virginia, Attn: Mr. I. E. Garrick.
1	Director, Langley Research Center, Langley Station, Hampton, Virginia, Attn: Mr. D. J. Marten.
1	Director, Engineering Science Division, National Science Foundation, Washington, D. C.
1	Director, National Bureau of Standards, Washington 25, D. C., Attn: Mr. J. M. Franklin.
1	Dr. G. B. Schubauer, Fluid Mechanics Section, National Bureau of Standards, Washington 25, D. C.
20	Defense Documentation Center, Cameron Station, Alexandria, Virginia.
1	Office of Technical Services, Department of Commerce, Washington 25, D. C.
1	Mr. Alfonso Alcadan L., Director, Laboratorio Nacional de Hydraulica, Antiguo Camino A Ancon, Casialla Postal, 682, Lima, Peru.
1	Mr. T. A. Duncan, Lycoming Division, AVCO Corporation, 1701 K Street, NW, Apartment 904, Washington, D. C.

Copies	Organization
1	Baker Manufacturing Company, Evansville, Wisconsin.
1	Professor S. Siestrunck, Bureau D'Analyse et de Recherche Appliquees, 47, Avenue Victor Cresson, Issy-les-Moulineaux, Seine, France.
1	Professor A. Acosta, California Institute of Technology, Pasadena 4, California.
1	Professor M. Plesset, California Institute of Technology, Pasadena 4, California.
1	Professor T. Y. Wu, California Institute of Technology, Pasadena 4, California.
1	Professor A. Powell, University of California, Los Angeles, California.
1	Dr. Maurice L. Albertson, Professor of Civil Engineering, Colorado State University, Fort Collins, Colorado 80521.
1	Professor J. E. Cermak, Colorado State University, Department of Civil Engineering, Fort Collins, Colorado.
1	Dr. Blaine R. Parkin, General Dynamics - Convair, P. O. Box 1950, San Diego 12, California.
1	Robert H. Oversmith, Chief of ASW/Marine Sciences, Mail Zone 6-107, General Dynamics - Convair, San Diego, California 92112.
1	Dr. Irving C. Statler, Head, Applied Mechanics Department, Cornell Aeronautical Laboratory, Inc., P.O. Box 235, Buffalo, New York 14221.
1	Mr. Richard P. White, Jr., Cornell Aeronautical Laboratory, 4455 Genesee Street, Buffalo, New York.
1	Professor W. R. Sears, Graduate School of Aeronautical Engineering, Cornell University, Ithaca, New York.
1	Mr. George H. Pedersen, Curtiss-Wright Corporation, Wright Aeronautical Division, Wood-Ridge, New Jersey, Location CC-1 Engrg. Mezz.
1	Mr. G. Tedrew, Food Machinery Corporation, P. O. Box 367, San Jose, California.
1	General Applied Science Laboratory, Merrick and Stewart Avenues, Westbury, Long Island, New York, Attn: Dr. Frank Lane.
1	Mr. R. McCandliss, Electric Boat Division, General Dynamics Corporation, Groton, Connecticut.
1	Dr. A. S. Iberall, President, General Technical Services, Inc., 2640 Whiton Road, Cleveland 18, Ohio.
1	Gibbs and Cox, Inc., 21 West Street, New York, New York 10006.
1	Mr. Eugene F. Baird, Chief of Dynamic Analysis, Grumman Aircraft Engineering Corporation, Bethpage Long Island, New York.

Copies	Organization
1	Mr. Robert E. Bower, Chief, Advanced Development, Grumman Aircraft Engineering Corporation, Bethpage, Long Island, New York.
1	Mr. William P. Carl, Grumman Aircraft Engineering Corporation, Bethpage, Long Island, New York.
1	Grumman Aircraft Engineering Corporation, Research Department, Plant 25, Bethpage, Long Island, New York 11714, Attn: Mr. Kenneth Keen.
1	Dr. O. Grim, Hamburgische Schiffbau - Versuchsanstalt, Bramfelder Strasse 164, Hamburg 33, Germany.
1	Dr. H. W. Lerbs, Hamburgische Schiffbau-Versuchsanstalt, Bramfelder Strasse 164, Hamburg 33, Germany.
1	Dr. H. Schwanecke, Hamburgische Schiffbau-Versuchsanstalt, Bramfelder Strasse 164, Hamburg 33, Germany.
1	Professor G. P. Weinblum, Director, Institute for Schiffbau, University of Hamburg, Berliner Tow 21, Hamburg, Germany.
1	Professor G. F. Carrier, Harvard University, Cambridge 38, Massachusetts.
1	Dr. S. F. Hoerner, 148 Busteed Drive, Midland Park, New Jersey.
1	Mr. P. Eisenberg, President, Hydronautics, Incorporated, Pindell School Road, Howard County, Laurel, Maryland.
1	Professor Carl Prohaska, Hydro-og Aerodynamisk Laboratorium, Lyngby, Denmark.
1	Professor L. Landweber, Iowa Institute of Hydraulic Research, State University of Iowa, Iowa City, Iowa.
1	Professor H. Rouse, Iowa Institute of Hydraulic Research, State University of Iowa, Iowa City, Iowa.
1	Professor S. Corrsin, Department of Mechanics, The Johns Hopkins University, Baltimore 18, Maryland.
2	Professor O. M. Phillips, Division of Mechanical Engineering, Institute for Cooperative Research, The Johns Hopkins University, Baltimore 18, Maryland.
1	Mr. Bill East, Lockheed Aircraft Corporation, California Division, Hydrodynamics Research, Burbank, California.
1	Mr. R. W. Kermeen, Lockheed Missiles and Space Company, Department 81-73/Bldg. 538, P. O. Box 504, Sunnyvale, California.
1	Department of Naval Architecture and Marine Engineering, Room 5-228, Massachusetts Institute of Technology, 77 Massachusetts Avenue, Cambridge 39, Massachusetts.
1	Professor M. A. Abkowitz, Massachusetts Institute of Technology, Cambridge 39, Massachusetts.

Copies	Organization
1	Professor H. Ashley, Massachusetts Institute of Technology, Cambridge 39, Massachusetts.
1	Professor A. T. Ippen, Massachusetts Institute of Technology, Cambridge 39, Massachusetts.
1	Professor M. Landahl, Massachusetts Institute of Technology, Cambridge 39, Massachusetts.
1	Dr. H. Reichardt, Director, Max-Planck Institut fur Stromungsforschung, Bottingerstrasse 6-8, Gottingen, Germany.
1	Professor R. B. Couch, University of Michigan, Ann Arbor, Michigan.
1	Professor W. W. Willmarth, University of Michigan, Ann Arbor, Michigan.
1	Midwest Research Institute, 425 Volker Boulevard, Kansas City, Missouri, Attn: Library.
1	Director, St. Anthony Falls Hydraulic Laboratory, University of Minnesota, Minneapolis 14, Minnesota.
1	Mr. C. S. Song, St. Anthony Falls Hydraulic Laboratory, University of Minnesota, Minneapolis 14, Minnesota.
1	Mr. J. M. Wetzel, St. Anthony Falls Hydraulic Laboratory, University of Minnesota, Minneapolis 14, Minnesota.
1	Head, Aerodynamics Division, National Physical Laboratory, Teddington, Middlesex, England.
1	Mr. A. Silverleaf, National Physical Laboratory, Teddington, Middlesex, England.
1	The Aeronautical Library, National Research Council, Montreal Road, Ottawa 2, Canada.
1	Dr. J. B. Van Manen, Netherlands Ship Model Basin, Wangeningen, The Netherlands.
1	Professor John J. Foody, Chairman, Engineering Department, State University of New York, Maritime College, Bronx, New York 10465.
1	Professor J. Keller, Institute of Mathematical Sciences, New York University, 25 Waverly Place, New York 3, New York.
1	Professor J. J. Stoker, Institute of Mathematical Sciences, New York University, 25 Waverly Place, New York 3, New York.
1	Dr. T. R. Goodman, Oceanics, Incorporated, Technical Industrial Park, Plainview, Long Island, New York.
1	Professor J. William Holl, Department of Aeronautical Engineering, The Pennsylvania State University, Ordnance Research Laboratory, P. O. Box 30, State College, Pennsylvania.
1	Dr. M. Sevik, Ordnance Research Laboratory, Pennsylvania State University, University Park, Pennsylvania.

Copies	Organization
1	Dr. George F. Wislicenus, Garfield Thomas Water Tunnel, Ordnance Research Laboratory, The Pennsylvania State University, Post Office Box 30, State College, Pennsylvania 16801.
1	Professor E. J. Brunelle, Princeton University, Princeton, New Jersey.
1	Mr. David Wellinger, Hydrofoil Projects, Radio Corporation of America, Burlington, Massachusetts.
1	The RAND Corporation, 1700 Main Street, Santa Monica, California, 90406, Attn: Library.
1	Professor R. C. DiPrima, Department of Mathematics, Rensselaer Polytechnic Institute, Troy, New York.
1	Mr. L. M. White, U. S. Rubber Company, Research and Development Department, Wayne, New Jersey.
1	Professor J. K. Lunde, Skipsmodelltanken, Trondheim, Norway.
1	Editor, Applied Mechanics Review, Southwest Research Institute, 8500 Culebra Road, San Antonio 6, Texas.
1	Dr. H. N. Abramson, Southwest Research Institute, 8500 Culebra Road, San Antonio 6, Texas.
1	Mr. G. Ransleben, Southwest Research Institute, 8500 Culebra Road, San Antonio 6, Texas.
1	Professor E. Y. Hsu, Stanford University, Stanford, California.
1	Dr. Byrne Perry, Department of Civil Engineering, Stanford University, Stanford, California 94305.
1	Mr. J. P. Breslin, Stevens Institute of Technology, Davidson Laboratory, Hoboken, New Jersey.
1	Mr. D. Savitsky, Stevens Institute of Technology, Davidson Laboratory, Hoboken, New Jersey.
1	Mr. S. Tsakonas, Stevens Institute of Technology, Davidson Laboratory, Hoboken, New Jersey.
1	Dr. Jack Kotik, Technical Research Group, Inc., Route 110, Melville, New York.
1	Dr. R. Timman, Department of Applied Mathematics, Technological University, Julianalaan, Delft, 132, Holland.
1	Transportation Technical Research Institute, No. 1057-1 Chome, Mejiro-machi, Toshima-ku, Tokyo-to, Japan.
1	Dr. Grosse, Versuchsanstalt fur Wasserbau und Schiffbau, Schleuseninsel im Tiergarten, Berlin, Germany.
1	Dr. S. Schuster, Director, Versuchsanstalt fur Wasserbau und Schiffbau, Schleusensinsel im Tiergarten, Berlin, Germany.

Copies	Organization
1	Technical Library, Webb Institute of Naval Architecture, Glen Cove, Long Island, New York.
1	Professor E. V. Lewis, Webb Institute of Naval Architecture, Glen Cove, Long Island, New York.
1	Mr. C. Wigley, Flat 103, 6-9 Charterhouse Square, London E. C. 1, England.
1	Coordinator of Research, Maritime Administration, 441 G Street, NW, Washington 25, D. C.

Unclassified
Security Classification

DOCUMENT CONTROL DATA - R&D

(Security classification of title, body of abstract and indexing annotation must be entered when the overall report is classified)

1. ORIGINATING ACTIVITY *(Corporate author)*
St. Anthony Falls Hydraulic Laboratory, University of Minnesota

2a. REPORT SECURITY CLASSIFICATION
Unclassified

2b. GROUP

3. REPORT TITLE
FURTHER STUDIES OF VENTILATED CAVITIES ON SUBMERGED BODIES

4. DESCRIPTIVE NOTES *(Type of report and inclusive dates)*
Interim Report

5. AUTHOR(S) *(Last name, first name, initial)*
Schiebe, Frank R.
Wetzel, Joseph M.

6. REPORT DATE	7a. TOTAL NO. OF PAGES	7b. NO. OF REFS
October 1964	50	14

8a. CONTRACT OR GRANT NO.	9a. ORIGINATOR'S REPORT NUMBER(S)
Nonr 710(48)	Project Report No. 72
b. PROJECT NO. NR 062-192	
c.	9b. OTHER REPORT NO(S) *(Any other numbers that may be assigned this report)*
d.	

10. AVAILABILITY/LIMITATION NOTICES
Qualified requestors may obtain copies of this report from DDC.

11. SUPPLEMENTARY NOTES	12. SPONSORING MILITARY ACTIVITY
	Office of Naval Research

13. ABSTRACT

Experimental studies were conducted to determine the air requirements of ventilated cavities on finite-span hydrofoils and other submerged bodies near a free surface. Reentrant jet, trailing vortex, and pulsating cavities were observed. Semi-empirical equations for predicting the air requirements for reentrant jet and trailing vortex cavities are presented. The transition region between reentrant jet and trailing vortex cavities was also investigated. For some conditions, pulsating cavities were found in the transition region.

DD FORM 1 JAN 64 1473 0101-807-6800

Unclassified
Security Classification

14. KEY WORDS	LINK A		LINK B		LINK C	
	ROLE	WT	ROLE	WT	ROLE	WT
Hydrofoils						
Ventilation						
Steady Flow						
Free-Surface Effects						
Three-Dimensional Foils						

INSTRUCTIONS

1. ORIGINATING ACTIVITY: Enter the name and address of the contractor, subcontractor, grantee, Department of Defense activity or other organization *(corporate author)* issuing the report.

2*a*. REPORT SECURITY CLASSIFICATION: Enter the overall security classification of the report. Indicate whether "Restricted Data" is included. Marking is to be in accordance with appropriate security regulations.

2*b*. GROUP: Automatic downgrading is specified in DoD Directive 5200.10 and Armed Forces Industrial Manual. Enter the group number. Also, when applicable, show that optional markings have been used for Group 3 and Group 4 as authorized.

3. REPORT TITLE: Enter the complete report title in all capital letters. Titles in all cases should be unclassified. If a meaningful title cannot be selected without classification, show title classification in all capitals in parenthesis immediately following the title.

4. DESCRIPTIVE NOTES: If appropriate, enter the type of report, e.g., interim, progress, summary, annual, or final. Give the inclusive dates when a specific reporting period is covered.

5. AUTHOR(S): Enter the name(s) of author(s) as shown on or in the report. Enter last name, first name, middle initial. If military, show rank and branch of service. The name of the principal author is an absolute minimum requirement.

6. REPORT DATE: Enter the date of the report as day, month, year; or month, year. If more than one date appears on the report, use date of publication.

7*a*. TOTAL NUMBER OF PAGES: The total page count should follow normal pagination procedures, i.e., enter the number of pages containing information.

7*b*. NUMBER OF REFERENCES: Enter the total number of references cited in the report.

8*a*. CONTRACT OR GRANT NUMBER: If appropriate, enter the applicable number of the contract or grant under which the report was written.

8*b*, 8*c*, & 8*d*. PROJECT NUMBER: Enter the appropriate military department identification, such as project number, subproject number, system numbers, task number, etc.

9*a*. ORIGINATOR'S REPORT NUMBER(S): Enter the official report number by which the document will be identified and controlled by the originating activity. This number must be unique to this report.

9*b*. OTHER REPORT NUMBER(S): If the report has been assigned any other report numbers *(either by the originator or by the sponsor)*, also enter this number(s).

10. AVAILABILITY/LIMITATION NOTICES: Enter any limitations on further dissemination of the report, other than those imposed by security classification, using standard statements such as:

(1) "Qualified requesters may obtain copies of this report from DDC."

(2) "Foreign announcement and dissemination of this report by DDC is not authorized."

(3) "U. S. Government agencies may obtain copies of this report directly from DDC. Other qualified DDC users shall request through _____."

(4) "U. S. military agencies may obtain copies of this report directly from DDC. Other qualified users shall request through _____."

(5) "All distribution of this report is controlled. Qualified DDC users shall request through _____."

If the report has been furnished to the Office of Technical Services, Department of Commerce, for sale to the public, indicate this fact and enter the price, if known.

11. SUPPLEMENTARY NOTES: Use for additional explanatory notes.

12. SPONSORING MILITARY ACTIVITY: Enter the name of the departmental project office or laboratory sponsoring *(paying for)* the research and development. Include address.

13. ABSTRACT: Enter an abstract giving a brief and factual summary of the document indicative of the report, even though it may also appear elsewhere in the body of the technical report. If additional space is required, a continuation sheet shall be attached.

It is highly desirable that the abstract of classified reports be unclassified. Each paragraph of the abstract shall end with an indication of the military security classification of the information in the paragraph, represented as *(TS), (S), (C), or (U)*.

There is no limitation on the length of the abstract. However, the suggested length is from 150 to 225 words.

14. KEY WORDS: Key words are technically meaningful terms or short phrases that characterize a report and may be used as index entries for cataloging the report. Key words must be selected so that no security classification is required. Identifiers, such as equipment model designation, trade name, military project code name, geographic location, may be used as key words but will be followed by an indication of technical context. The assignment of links, roles, and weights is optional.